CNWRA®
A center of excellence in earth sciences and engineering®

Geosciences and Engineering Division
6220 Culebra Road • San Antonio, Texas, U.S.A. 78238-5166
(210) 522-5160 • Fax (210) 522-5155

March 29, 2012
Contract No. NRC-02-07-006
Account No. 20.14003.01.072
PROJ0734; PROJ0735
NMCF1

ATTN: Document Control Desk
U.S. Nuclear Regulatory Commission
Mr. Mathews George
Division of Waste Management and Environmental Protection
FSME/DWMEP/EPPAD
Mail Stop 8-F8
11555 Rockville Pike
Rockville, MD 20852

Subject: Revised Final Progress Report: Experimental Study of Contaminant Release From Reducing Grout (Deliverable 14003.01.007.475)

Dear Mr. George:

This letter transmits a revised version of the Final Progress Report: Experimental Study of Contaminant Release from Reducing Grout that was transmitted to NRC on December 28, 2011. The work described in the report was undertaken to better inform the U.S. Nuclear Regulatory Commission (NRC) understanding of radionuclide release from grouted waste forms the U.S. Department of Energy is producing for the Savannah River Site Saltstone Disposal Facility. The report was revised in response to NRC staff comments that were transmitted to the CNWRA on January 20, 2012. The revisions that were incorporated into the report have been discussed with NRC staff.

Please let me know of additional NRC comments or suggestions on this report. We look forward to continuing to support NRC work in this important area with additional experiments and related analysis and interpretations. Please do not hesitate to contact me (210.522.6418) or Dr. Roberto Pabalan (210.522.5304) with any questions about the subject report.

Sincerely,

Robert J. Lenhard, Ph.D.
Program Manager
Environmental Protection and Waste
Management for Non-High Level
Radioactive Waste

RL/RP/ls
cc:
D. DeMarco
R. Jackson
V. Whipple
A. Persinko
G. Suber
C. Barr
C. McKenney
N. Devaser
J. Shaffner
G. Alexander
W. Patrick
B. Sagar
GED Directors/Managers
R. Pabalan
D. Waiting
Record Copy B—IQS
M. Padilla

Washington Office
1801 Rockville Pike, Suite 105 • Rockville, Maryland 20852-1633

EXPERIMENTAL STUDY OF CONTAMINANT RELEASE FROM REDUCING GROUT

Prepared for

U.S. Nuclear Regulatory Commission
Contract NRC–02–07–006

Prepared by

R.T. Pabalan[1]
G.W. Alexander[2]
D.J. Waiting[1]

[1]Center for Nuclear Waste Regulatory Analyses
San Antonio, Texas

[2]U.S. Nuclear Regulatory Commission
Washington, DC

March 2012

CONTENTS

FIGURES

FIGURES (continued)

Figure Page

TABLES

EXECUTIVE SUMMARY

The ability of cement-based materials (e.g., grout) to serve as barriers to groundwater influx and to radionuclide release and transport is an important factor in U.S. Department of Energy (DOE) performance assessments. These performance assessments are conducted to demonstrate that tank closure and low-activity waste disposal in near-surface disposal facilities will meet the appropriate performance objectives. In these performance assessments, assumptions are made regarding the physical integrity and chemical condition of the cement-based material. For redox-sensitive radioelements (e.g., technetium, neptunium, uranium, and selenium), a key factor determining their release and transport is the redox potential of the cement-based material. Various studies have demonstrated that grouted systems containing blast furnace slag are effective in mitigating the release of redox-sensitive radioelements. However, there are uncertainties in the reductive capacity of slag-bearing grouts, the long-term persistence of their reducing capabilities, and their ability to mitigate the release of redox-sensitive radioelements.

In this study, two types of experiments were conducted to determine the release behavior of the redox-sensitive radioelements technetium, uranium, and selenium initially sequestered in reducing grout as water interacted with the grout and changed the system chemistry. One type of experiment flowed oxygen-bearing simulated Savannah River Site (SRS) groundwater through a column of crushed and sieved simulated SRS saltstone material and monitored the changes in pH, Eh, and aqueous concentrations. Results from this experiment showed that significant changes in system chemistry occurred during the first 10 to 14 pore volumes of simulated SRS groundwater flow through the column. The effluent solution pH decreased relatively quickly from 12.9 to ~11.8 during the first 14 pore volumes, then decreased much more slowly, reaching only 11.1 after 134 pore volumes. No pH buffering at 12.5 was observed, indicating portlandite did not form in significant amounts in the grout to buffer the pH at that value. The Eh quickly increased from a low value of –453 mV to positive Eh values with as few as 12 pore volumes of solution flow and then increased more gradually afterward. In one of the two column experiments (Cell 1), a sudden 120-mV increase in Eh was observed after 46 pore volumes, but this sudden Eh increase was not observed in the other column experiment (Cell 2).

Technetium release from the simulated saltstone increased sharply during the first 10 pore volumes, increased more gradually until 52 pore volumes in Cell 1 or 26 pore volumes in Cell 2 were reached, then afterwards increased significantly with increasing pore volume. The technetium that was released early likely represents technetium that was not effectively immobilized in the reducing grout or technetium that was reoxidized during the crushing and sieving of the grout material. The significant increase in technetium release observed in Cell 1 after 52 pore volumes and in Cell 2 after 26 pore volumes is slightly delayed relative to the Eh increase observed in both cells. The technetium cumulative fraction leached from Cell 1 was 0.04 at 52 pore volumes, but increased to 0.25 at 134 pore volumes. The technetium cumulative fraction leached from Cell 2 was 0.10 at 26 pore volumes and increased to 0.19 at 132 pore volumes. The data show that uranium is retained in the reducing grout, whereas almost all of the selenium is released after 132 pore volumes. A posttest analysis of the Cell 1 grout that was extruded from the flow cell indicated that the fraction of technetium leached from the grout decreased from ~0.64 near the column inlet to ~0.46 near the column outlet. These values are higher than the Cell 1 value of 0.25 at 134 pore volumes that was derived from the technetium concentration in the effluent solutions. The latter value is lower probably because the periodic sampling of effluent solutions missed short periods of high technetium fractional release, such as during the onset of the experiment or following the Eh transition. Notwithstanding the differences in the calculated technetium leached fraction, the data indicate

that much of the technetium originally present in the column remained in a reduced, low solubility phase. This is consistent with a mass balance analysis that showed the amount of dissolved O_2 which has flowed through the column would have consumed only a fraction of the reducing capacity of the grout.

An Eh–pH diagram indicates the system chemistry in the column experiment started under conditions in which technetium solubility is low, constrained by Tc_3O_4 solubility, but eventually transitioned into the stability field of the pertechnetate ion. Although this transition should have corresponded to a significant increase in technetium release, it was not observed in the experiment. Instead, an increase in technetium release occurred later than the observed Eh increase and at a slower rate than expected based on the change in solution chemistry. The time lag between Eh increase and technetium release possibly is due to slow oxidation of technetium at depth within the grout particles, which in turn is likely controlled by oxygen diffusion into the particles. Based on literature information, an alternative explanation is the formation of a low solubility, likely metastable Tc(IV) phase, which is resistant to oxidative remobilization. In contrast to technetium, selenium release was not solubility limited. An Eh–pH diagram of selenium speciation indicates that under the initial Eh–pH conditions, selenium likely was present as an aqueous HSe^- species. Given that selenium release does not appear to be transport limited, release of technetium, once soluble, also is unlikely to be transport limited.

The second type of experiment leached cylindrical specimens of simulated saltstone material—one set cured at room temperature and another at 60 °C [140 °F]—in oxygen-bearing deionized water and monitored aqueous concentrations over time. Qualitatively, the data indicate that the leach rates for the different species increase in the order technetium < nitrate ≈ nitrite < selenium. Measured uranium concentrations were mostly below the inductively coupled plasma–mass spectrometry detection limit, indicating uranium was not released from the reducing grout within the timeframe of the experiment. Data analysis using the ALT computer program indicated the leaching data were generally consistent with a diffusion release mechanism. A more likely release mechanism involves both chemical reaction (e.g., oxidative dissolution) and diffusion, which is not a model option in the ALT program. Effective diffusion coefficients on the order of 10^{-11} cm^2/s [1.6×10^{-12} in^2/s] were derived for technetium, nitrate, and nitrite, approximately 10^{-10} cm^2/s [1.6×10^{-11} in^2/s] for selenium and approximately 10^{-9} cm^2/s [1.6×10^{-10} in^2/s] for sodium. The nitrate, nitrite, selenium, and sodium effective diffusion coefficients are higher for the grout cylinders cured at 60 °C [140 °F] compared to those cured at room temperature, but the technetium D_e is lower for the former than for the latter.

Due to the limited spatial and temporal scale and range of parameters (e.g., particle or monolith size, flow rate) used in the experiments, care should be taken when extrapolating the results to actual field conditions. A full-scale system will have flow geometries, flow rates, and reactive surface areas that will vary spatially and temporally. Reaction kinetics also will affect the evolution of the system chemistry. To enable extrapolation of experimental results to longer time frames and larger spatial scales, as well as facilitate an evaluation of the effect of varying chemical (e.g., solution composition) and physical (e.g., particle size, surface area, flow rate) parameters on contaminant release, reactive transport modeling of contaminant leaching could be conducted. As the range of parameters in these experiments was limited, additional experiments varying the particle size and/or flow rate would be useful. In addition, because the physical and chemical conditions in actual saltstone waste and the release behavior of

radionuclides could be different than those in the laboratory experiments, leaching experiments using actual SRS saltstone samples are strongly recommended.

ACKNOWLEDGMENTS

This report was prepared to document work performed by the Center for Nuclear Waste Regulatory Analyses (CNWRA®) for the U.S. Nuclear Regulatory Commission (NRC) under Contract No. NRC–02–07–006. The activities reported here were performed on behalf of the NRC Office of Federal and State Materials and Environmental Management Programs, Division of Waste Management and Environmental Protection. This report is an independent product of CNWRA and does not necessarily reflect the view or regulatory position of NRC. The NRC staff views expressed herein are preliminary and do not constitute a final judgment or determination.

The authors wish to thank J. Myers and NRC staff for their technical review, E. Pearcy for his programmatic review, L. Mulverhill for her editorial review, and L. Selvey for her secretarial support. F.P. Bertetti is also thanked for performing the Tc-99 liquid scintillation analyses.

QUALITY OF DATA, ANALYSES, AND CODE DEVELOPMENT DATA

DATA: All CNWRA-generated data contained in this report meet quality assurance requirements described in the Geosciences and Engineering Division Quality Assurance Manual. Sources of other data should be consulted for determining the level of quality of those data.

ANALYSES AND CODES: This report includes results of calculations performed using Geochemist's Workbench® (Bethke and Yeakel, 2007). Data reduction and plotting were accomplished using Microsoft® Excel® (Microsoft® Corporation, 2002) and Sigmaplot® (Systat Software, Inc., 2008). The work presented in this report is documented in Scientific Notebook 1019E (Pabalan, 2010).

References:

Bethke, C.M. and S. Yeakel. "Geochemist's Workbench® Release 7.0." Golden, Colorado: RockWare, Inc. 2007.

Microsoft® Corporation. "Excel®." Redland, Washington: Microsoft® Corporation. 2002.

Pabalan, R.T. "Column Experiments on Technetium-99 Leaching From Simulated Saltstone Grout." Scientific Notebook 1019E. San Antonio, Texas: CNWRA. pp. 1–327. 2010.

Systat Software, Inc. "Sigmaplot® 11." San Jose, California: Systat Software, Inc. 2008.

1 INTRODUCTION

The ability of cement-based materials (e.g., grout) to serve as barriers to groundwater influx and to radionuclide release and transport is an important factor in U.S. Department of Energy (DOE) performance assessments. These performance assessments are conducted to demonstrate that tank closure and low-activity waste disposal in near-surface disposal facilities will meet the appropriate performance objectives. In these performance assessments, assumptions are made regarding the physical integrity and chemical condition of the cement-based material. For redox-sensitive radioelements (e.g., technetium, neptunium, uranium, and selenium), a key factor determining their release and transport is the redox potential of the cement-based material (DOE-Idaho, 2003; Savannah River Remediation Closure and Waste Disposal Authority, 2009; Pabalan, et al., 2009).

Various studies have demonstrated that grouted systems containing blast furnace slag are effective in mitigating the release of redox-sensitive radionuclides such as Tc-99 (Langton, 1987; Brodda, 1988; Gilliam, et al., 1988; Cook and Fowler, 1992; Aloy, et al., 2007). Hydration of the blast furnace slag in the grout mixture releases sulfide species into the pore fluid, predominantly as S^{2-}, which impose a strongly reducing redox potential (Eh) on the system (Atkins and Glasser, 1992). At low Eh conditions, the solubilities of redox-sensitive elements tend to be low (Angus and Glasser, 1985; Ewart, et al., 1992; Pickett, et al., 2009). Also, sulfide species released into solution by slag hydration can chemically bind some contaminants as insoluble species. For example, technetium is believed to react with the sulfide to form relatively insoluble TcS_2 (Allen, et al., 1997), Tc_3S_{10} (Lukens, et al., 2005), or Tc_2S_7 (Liu, et al., 2007).

Existing national standards do not specify the sulfide content of slag, except as a maximum, and commercial blast furnace slag may vary in the amount of sulfide. Most North American and European slag contains sulfur (as sulfide) in the range 0.6 to 1.0 weight percent (wt%) (Pabalan, et al., 2009), but the modern tendency to use preprocessed iron feed stocks and "clean" coals results in the sulfur content of modern slag tending toward lower values. As a consequence, there are uncertainties in the amount of sulfide and in the reductive capacity of slag-bearing grouts.

In addition, there is uncertainty regarding the long-term persistence of the reducing capabilities of the slag-bearing grout. Oxygen (O_2) in the gas phase or dissolved in infiltrating water could react with and decrease the reductive capacity of slag. Calculations have been performed on O_2 oxidation of reducing grout to evaluate the longevity of low Eh conditions of grouted systems for radioactive waste disposal (Kaplan, et al., 2005; Kaplan and Hang, 2007; Denham, 2008; Painter and Pabalan, 2009). For example, Denham (2008) calculated the changes in pore fluid Eh and pH as a function of the number of pore volumes of groundwater infiltrate that react with the concrete and grout minerals. Denham (2008) calculated that the Eh transition from –0.45 V to about +0.6 V will occur for the slag-bearing grout at around 2,800 pore volumes. The pH transition from 11.0 to less than 10 was calculated to occur at pore volumes ranging from 2,300 to 10,400, depending on the initial pH of the groundwater infiltrate. However, little experimental data are available for comparison with the calculated results and for correlating the changes in grout system chemistry with radionuclide release.

In this study, experiments on contaminant release from reducing grout were conducted. This report discusses the materials and methods used in the experiment and presents data on the evolution of system chemistry and contaminant release. The objective of the study was to determine the oxidative dissolution and release behavior of redox-sensitive radioelements initially sequestered in reducing grout as oxygen-bearing water interacts with the grout and

changes the system chemistry. Of particular interest is the amount of contaminant released from the grout as the fluid pH and the system Eh evolve. The expected changes in pH and Eh can be described as follows. At the earliest stages, the cement pore fluid pH is expected to be greater than 13 due to the presence of the soluble alkalis sodium and potassium. This stage is likely short in duration as percolating water rapidly leaches the alkalis. If portlandite [$Ca(OH)_2$] is present in significant amounts in the grout, the percolating water subsequently will have a pH of about 12.5 buffered by portlandite dissolution. When portlandite dissolution is complete, leaching of amorphous to poorly crystalline calcium silicate hydrate (C-S-H) will continue and the pH will begin to decline to about 10.5. Once C-S-H is exhausted, carbonate phases such as calcite likely will be abundant and control pH to about 8. The system Eh is expected to be initially low, with technetium, uranium, and selenium likely present in a tetravalent oxidation state (Tc^{IV}, U^{IV}, and Se^{IV}). The system Eh is expected to progressively increase as dissolved O_2 reacts with the grout. Contaminant release is expected to also increase as the system becomes progressively more oxidizing and technetium, uranium, and selenium are converted to more soluble and/or less sorbing oxidation states (Tc^{VII}, U^{VI}, and Se^{VI}). The rate at which the pH and Eh change is expected to be a function of the amount of water that reacts with the grout.

The study focused on contaminant release from grout that has a composition similar to Savannah River Site (SRS) saltstone. Saltstone is a cementitious waste form made by mixing salt solution originating from SRS liquid waste storage tanks with a dry mix containing blast furnace slag, fly ash, and Portland cement (Savannah River Remediation Closure and Waste Disposal Authority, 2009). Solidified saltstone is a dense, alkaline, reducing, microporous, monolithic, cementitious matrix containing a salt solution within its pore structure. Technetium, uranium, and selenium were included in the experiments because they were found to be important risk drivers in some performance assessment calculations (e.g., Kaplan, et al., 2008; Savannah River Remediation Closure and Waste Disposal Authority, 2009).

Two types of contaminant release experiments were conducted: (i) flowing oxygen-bearing simulated SRS groundwater through a column of crushed and sieved simulated saltstone material and monitoring the solution pH, Eh, contaminant concentration, and other chemical parameters over time and (ii) leaching cylindrical specimens of simulated saltstone material in oxygen-bearing deionized water and monitoring the released contaminant concentration over time. In the former type of experiment, contaminant release likely will be controlled by oxygen diffusion into the reducing grout particles; oxidative dissolution of tetravalent technetium, uranium, and selenium in the grout; diffusion of the dissolved contaminants out of the grout particles; and advective transport out of the column. In the latter type of experiment, oxygen diffusion into the grout cylinder, oxidative dissolution of the contaminant, and contaminant diffusion out of the grout also will be important. Because of the much shorter grout material diffusion lengths in the former versus the latter, contaminant release is expected to be higher in the column experiment than in the cylinder leaching experiment. Also, it is possible a fraction of the contaminants will not have been immobilized effectively in the reducing grout and could be released early, particularly in the column experiment where partial oxidation of the tetravalent contaminants could occur during the preparation of the crushed and sieved grout material. Immobilization of a contaminant also could occur (e.g., coprecipitation with calcite) as it is transported along the column length; this may need to be considered in data interpretation.

Column experiments represent a dynamic system that can provide valuable information on the long-term evolution of a system being simulated, including changes in chemistry over time based on depletion of buffering components in the saltstone grout. Data from this type of experiment, when parameterized in terms of pore volumes, can be extrapolated to long times using groundwater modeling estimates of the number of pore volumes per year expected to flow

through a system. In this way, contaminant release from SRS saltstone can be modeled as a function of time if reaction rates can be demonstrated to be fast relative to flow rates. The grout cylinder leaching experiments can provide information on (i) diffusion coefficients, (ii) sorption coefficients, and (iii) fraction released over time for an intact saltstone monolith during the early stages of leaching (e.g., under reducing conditions). The data may be extrapolated to estimate the leach rates of larger specimens (with longer diffusion lengths) or a bigger number of blocks (representing increased surface area or smaller diffusion lengths) that could occur due to degradation and cracking.

Note that due to the spatial and temporal scaling required to conduct these experiments in a laboratory setting and the limited range of parameters (e.g., particle or monolith size, flow rate) used in the experiments, care should be taken when extrapolating the results to actual field conditions. A full-scale system will have flow geometries, flow rates, and reactive surface areas that will vary spatially and temporally. Reaction kinetics also will affect the evolution of the system chemistry, including pH and Eh. Thus, the chemistry of a full-scale system may evolve much differently from that which can be observed in the laboratory scale experiments conducted in this study. In addition, the chemical form of the radionuclides in the simulated saltstone used in this study may be different than in an actual saltstone waste form. Thus, the leaching behavior of radionuclides from a simulated saltstone may be different than from an actual saltstone waste form.

2 MATERIALS AND METHODS

2.1 Simulated Saltstone

Simulated saltstone was prepared from dry solids components (Portland cement, fly ash, and blast furnace slag) and a non-radioactive simulant of SRS tank waste solution. The weight percentage of cement, fly ash, and slag in the dry mix is 10, 45, and 45, respectively, and the saltstone nominal blend composition is 5 wt% cement, 25 wt% fly ash, 25 wt% blast furnace slag, and 45 wt% salt solution (Savannah River Remediation Closure and Waste Disposal Authority, 2009). The recipe and formulation used to prepare the simulated saltstone were taken from Kaplan, et al. (2008), which provided recipes and formulations for the three SRS waste stream types: (i) Deliquifaction, Dissolution, and Adjustment (DDA); (ii) Salt Waste Processing Facility, and (iii) Modular Caustic Side Solvent Extraction Unit. The DDA simulant recipe and formulation were used in this study because DOE considered them to be representative of most of the waste streams going to the SRS Saltstone Facility (Kaplan, et al., 2008). The recipe and formulation are listed in Table 2-1. The DDA simulant solution was

Table 2-1. Recipe and Formulation for Deliquifaction, Dissolution, and Adjustment (DDA) Simulant Solution, Premix, and Simulated Saltstone*

DDA Simulant Components	Molarity	Molecular Weight (g/mol)	Amount per Liter Solution (g)
NaOH (50 wt% solution)	0.769	40.00	61.52
$NaNO_3$	2.202	84.99	187.15
$NaNO_2$	0.11	68.99	7.56
Na_2CO_3	0.145	105.99	15.36
Na_2SO_4	0.044	142.04	6.31
$Al(NO_3)_3{\cdot}9H_2O$	0.071	375.13	26.63
$Na_3PO_4{\cdot}12H_2O$	0.008	380.12	3.22
Premix Components		**Amount (g)**	
Blast Furnace Slag†		812	
Fly Ash		812	
Portland Cement		180	
Total		*1,804*	
Simulated Saltstone Components		**Amount (g)**	
Premix		1,804	
DDA Simulant Solution		1,396	

1 g = 3.5×10^{-2} oz

The 1,396 g of DDA simulant solution has 1,082 g of H_2O and 314 g of salt, giving a calculated water/cementitious material weight ratio of 0.6.

*Kaplan, D.I., K. Roberts, J. Coates, M. Siegfried, and S. Serkiz. "Saltstone and Concrete Interactions With Radionuclides: Sorption (K_d), Desorption, and Reduction Capacity Measurements." SRNS–STI–2008–00045. Aiken, South Carolina: Savannah River National Laboratory. 2008.

†There were two sources of blast furnace slag: LaFarge North America and Holcim, Inc. The LaFarge slag previously was used in Center for Nuclear Waste Regulatory Analyses (CNWRA) grout monolith experiments (Walter, G.R., C.L. Dinwiddie, E.J. Beverly, D. Bannon, D. Waiting, and G. Bird. "Mesoscale Grout Monolith Experiments: Results and Recommendations." San Antonio, Texas: CNWRA. 2009). The Holcim slag was obtained from Timothy Jones (Savannah River National Laboratory).

prepared from reagent grade chemicals using the amounts shown in Table 2-1. A dry premix was prepared by combining Portland cement, fly ash, and blast furnace slag in the amounts shown in the table and mixing in a plastic bag. Three batches of simulated saltstone were prepared: one with no contaminant; a second one containing Tc-99; and a third one containing Tc-99, U-238, and selenium. In preparing the second and third batches, a Tc-99 spike was added to the DDA simulant solution prior to mixing with the dry premix components. The Tc-99 spike, which was purchased from Eckert and Ziegler Analytics (Atlanta, Georgia), comprised 101.5 μCi {5.97×10^{-3} g [2.11×10^{-4} oz]} of Tc-99 {as ammonium pertechnetate [$NH_4{}^{99}Tc(VII)O_4$]} in 5 g [0.18 oz] of water. For the third batch of simulated saltstone, 60 mL [3.7 in^3] of a 0.05-M U-238 solution and 1.40 g [0.049 oz] of reagent grade K_2SeO_4 chemical also were added to the DDA simulant solution. The 0.05-M U-238 solution was prepared by dissolving reagent grade uranyl nitrate hexahydrate [$UO_2(NO_3)_2 \cdot 6H_2O$] in deionized water. The contaminant-bearing simulated saltstone was used in the column and cylinder leaching experiments, whereas the uncontaminated simulated saltstone was used for grout material characterization.[1]

To make each batch of simulated saltstone, the dry premix was placed in a Hobart mixer and blended using a flat beater agitator at low speed for several minutes. While still at low speed, the DDA simulant was added slowly (over a 30-second period) to the premix. Subsequently, the stirring rate was raised to the medium setting and mixing continued for an additional 2 minutes. Then the grout was poured into a cylindrical plastic mold {10.3-cm [4 1/16-in] inner diameter by 20.3-cm [8-in] length]}. The mold was capped and the grout allowed to cure for 28 days. The excess grout {~100 cm^3 [~6 in^3]} was placed in a plastic ziplock bag or in another capped plastic mold.

The batch that contained Tc-99, U-238, and selenium also was used to prepare cylindrical grout specimens. After being mixed in the Hobart mixer, portions of the still fluid simulated saltstone material were transferred into twenty-two 2.54-cm [1-in] inner diameter by 2.54-cm [1-in] length Teflon cylindrical molds, which were cut from a 1.83-m [6-ft] length Teflon pipe. The bottom of each mold was sealed with a Glad® Press'nSeal® plastic sealing wrap. A 17.8-cm [7-in] length of Teflon monofilament {0.089-cm [0.035-in] diameter} was threaded through the Press'nSeal wrap and secured with Scotch® tape. The cylindrical grout specimens were cured for 28 days inside two dessicators that have deionized water at the bottom to maintain a constantly humid environment. To determine any potential effect of curing temperature on contaminant release, one dessicator was maintained at room temperature and the other was placed in a laboratory oven with the temperature set at 60 °C [140 °F]. Laboratory studies at Savannah River National Laboratory (Harbour, et al., 2009) indicated that significant changes occur in the performance properties (e.g., porosity) of simulated saltstone samples when cured at 60 °C [140 °F].

After curing, the 10.3-cm [4 1/16-in] diameter by 20.3-cm [8-in] length contaminant-bearing simulated saltstone cylinders initially were broken up into 2.5- to 5-cm [1- to 2-in] pieces using a sledge hammer, then crushed with the aid of a Sepor (Sepor, Inc., Wilmington, California) mini-jaw crusher with a tungsten carbide jaw and cheek plates. The crushed material was dry sieved to the size range <35 and >140 mesh size {<0.50 and >0.105 mm [<0.0197 and >0.0041 in]} and stored in an N_2(g) atmosphere to minimize oxidation of the slag. The crushed and sieved material was used in the column experiments. The cured 2.54 by 2.54-cm [1 by 1-in] grout cylinders were gently extruded from the Teflon mold, and selected cylinders were used in the cylinder leaching experiment.

[1]LaFarge blast furnace slag was used in the first and second batches of simulated saltstone. Holcim slag was used in the third batch.

No attempt was made to keep an oxygen-free environment during preparation of the simulated saltstone cylinders and during crushing and sieving of the grout material for the column experiment. Significant oxidation of the reducing grout in the interior of the 2.54 by 2.54-cm [1 by 1-in] monoliths was unlikely before the experiment began because of slow oxygen diffusion into the monolith. However, the crushed and sieved grout material likely would have undergone a higher degree of oxidation than the monoliths before the experiment began, which may affect the contaminant release.

2.2 Simulated Savannah River Site Groundwater

Simulated SRS groundwater, with the composition listed in Table 2-2, was prepared from reagent grade chemicals using the recipe given in Table 2-3. Denham (2008) used a solution composition based on that listed in Table 2-2 to estimate the Eh and pH transitions in pore fluids during aging of SRS saltstone and disposal unit concrete that reacted with SRS groundwater. Because the simulated SRS groundwater is dilute {35 mg/L [35 ppm] total dissolved solids}, which is typical of SRS aquifer waters (Strom and Kaback, 1992), the chemistry of the column effluent solution is expected to be dominated by interaction of the solution with the grout material and contaminant release from the grout is expected to not change significantly if other SRS groundwater compositions had been used. The solution was not deaerated and was assumed to be O_2-saturated.

Table 2-2. Composition of Savannah River Site Groundwater Sample From Well P27D*

Ion	Concentration (mg/L)
Ca^{2+}	2.5
Mg^{2+}	0.41
Na^{+}	0.97
K^{+}	0.49
HCO_3^{-}	6
SO_4^{2-}	0.63
Cl^{-}	3.33

1 mg/L ≅ 1 ppm
*Strom, R.N. and D.S. Kaback. "SRP Baseline Hydrogeologic Investigation: Aquifer Characterization, Groundwater Geochemistry of the Savannah River Site and Vicinity." WSRC–RP–92–450. Aiken, South Carolina: Westinghouse Savannah River Company. 1992.

Table 2-3. Recipe for Preparing One Liter of Simulated Savannah River Site Groundwater With Composition Given in Table 2-2*

Reagent	Amount (g)
NaCl	2.47×10^{-3}
KCl	9.34×10^{-4}
$CaSO_4 \cdot 2H_2O$	2.25×10^{-3}
$MgCl_2 \cdot 6H_2O$	3.43×10^{-3}
$CaCl_2 \cdot 2H_2O$	7.25×10^{-3}

1 g = 3.5×10^{-2} oz; 1 L = 0.26 gal
*Bicarbonate reagent was excluded to simplify the recipe, but HCO_3^{-} is present in solution due to interaction with atmospheric CO_2(g). Because the solution is dilute, interactions with the saltstone simulant are expected to dominate the aqueous chemistry. To minimize errors in weighing reagents, a 100× concentrate was prepared as a stock solution.

2.3 Column Experiments

Two acrylic flow cells (Soil Measurement Systems, Tucson, Arizona) were dry loaded with crushed and sieved grout material (see Figure 2-1). The flow cells have a 3.8-cm [1.5-in] internal diameter, a 23-cm [9-in] length, and endplates with a porous nylon membrane. One cell (Cell 1) was loaded with Tc-99-bearing grout, whereas the other (Cell 2) was loaded with grout containing Tc-99, U-238, and selenium. The flow cells were tapped on the side intermittently to make the material packing denser. The calculated internal volume of the flow cells is 260 mL [15.9 in^3]. The total mass of grout loaded into Cell 1 was 209 g [7.4 oz], whereas 242 g [8.5 oz] of grout were loaded into Cell 2. The finer grain size of the grout material containing Tc-99, U-238, and selenium compared to the grout with Tc-99 only enabled more grout to be loaded into Cell 2. The finer grain size is indicated by the larger surface area measured for the former material compared to the latter (see Table 3-3).

Figure 2-2 is a photograph of the experimental setup. The simulated SRS groundwater was pumped from a 1-L [0.26-gal] solution reservoir upwards through the flow cell using an Agilent 1100 high-performance liquid chromatography (HPLC) pump. The flow rate was set at 0.066 mL/min [0.0040 in^3/min]. Downstream of the grout column, two acrylic, microflow cells (Lazar Research Laboratories, Los Angeles, California) were connected in series—one with a microflow-through pH electrode and the other with a microflow-through redox electrode. Both pH and redox electrodes have an epoxy electrode body, a Ag/AgCl (with 4-molar KCl solution) internal reference electrode, and internal volumes less than 50 µL. Downstream of the microflow cells, a 1-L [0.26-gal] Tedlar® bag (SKC, Inc., Eighty Four, Pennsylvania) was used to collect the effluent solutions. The Tedlar bag was replaced whenever it was almost full.

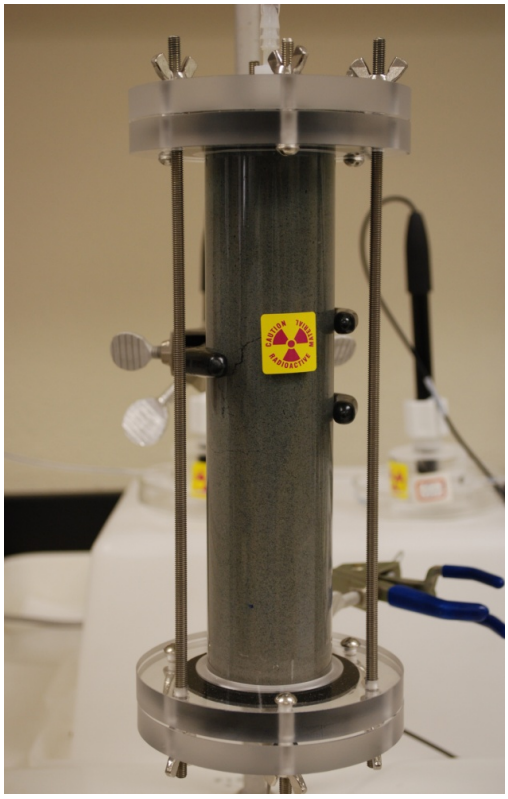

Figure 2-1. Acrylic Flow Cell With Contaminant-Bearing Simulated Saltstone Grout

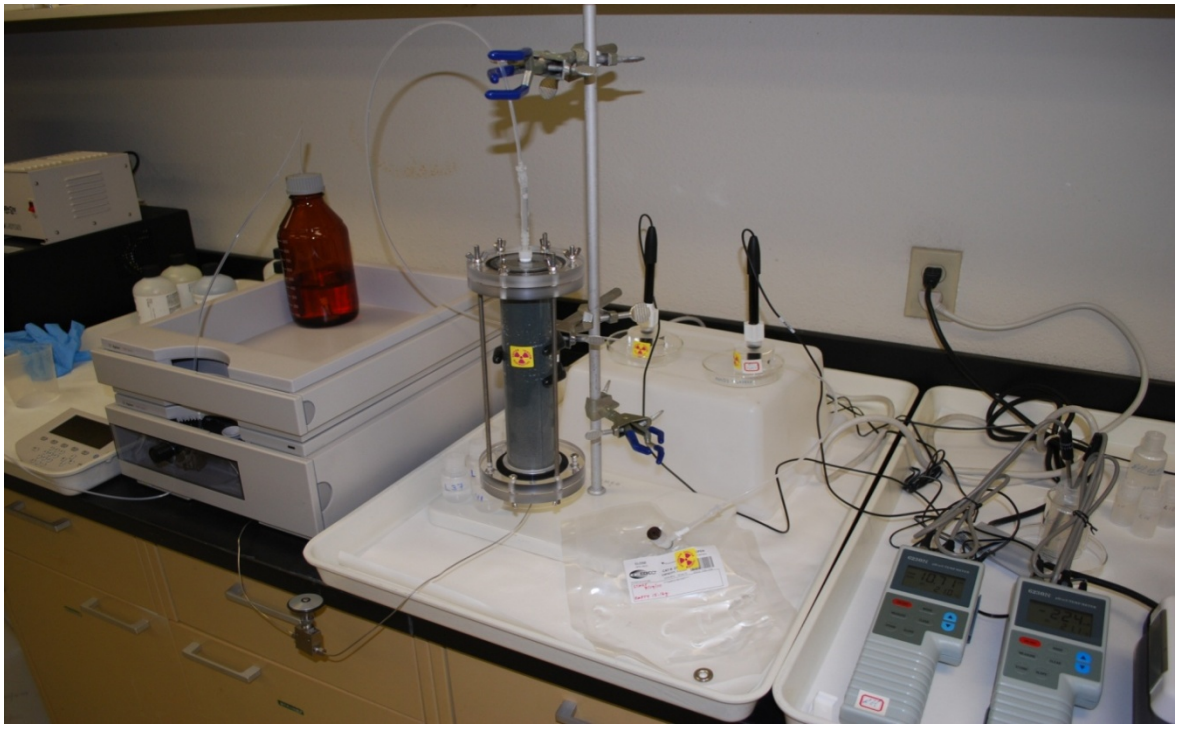

Figure 2-2. Column Experimental Setup

Aqueous samples for chemical analysis periodically were taken by disconnecting the Tedlar bag and allowing the solution to collect into a preweighed 15-, 30- or 50-mL [0.92-, 1.8- or 3.1-in^3] polypropylene bottle. Between 5- and 15-mL [0.31- and 0.92-in^3] samples were taken from Cell 1. Several of the samples were later combined to give a larger solution volume for chemical analysis. Larger volume {~50 mL [3.1 in^3]} samples were taken from Cell 2 to eliminate the need to combine samples for analysis. However, to collect 50-mL [3.1 in^3] samples in a reasonable amount of time, the pump flow rate was increased to 0.5 mL/min [0.031 in^3/min] during the sampling period. The bottles were reweighed after sampling to determine the sample mass. The Tedlar bag also was weighed each time a sample was taken or the bag replaced to enable the solution flow rate to be calculated. Two 1-mL [0.06-in^3] aliquots from each of the aqueous samples were taken to measure Tc-99 activity, and the remainder was preserved for later analysis of cation and anion concentration. The sample pH also was measured using an Orion ROSS combination pH electrode for comparison with the pH determined using the microflow-through pH electrode.

After completion of the Cell 1 column experiment, the grout in the flow cell was gently extruded and sliced into 14 sections. Three 0.25-g [0.0088-oz] samples were taken from each section—one from the center area and two from off-center areas of the section. Each sample was placed in a 15-mL [0.92-in^3] polypropylene bottle, and then 10 mL [0.61 in^3] of a 50 volume percent HNO_3 solution were added to each bottle to leach the residual technetium from the grout sample. The bottles were placed on a gyratory shaker for 2 days. Subsequently, two 1-mL [0.06-in^3] solution samples were taken from each bottle and analyzed for Tc-99 activity. Three 0.25-g [0.0088-oz] samples (sample names SSG-1, SSG-2, and SSG-3) of the unused grout material also were leached with HNO_3 solutions and the leachants analyzed for Tc-99

activity. These data will provide information on the relative distribution and approximate amount of technetium left in the grout column. To determine the effectiveness of technetium leaching by the 50 volume percent HNO_3 solution, the residual solids of the SSG samples and three additional samples of the unused and unreacted grout material were analyzed for Tc-99 activity.

In addition, during the later part of the Cell 2 experiment, the flow to the column was interrupted to allow a longer reaction time between the solution and reducing grout. After several days, the flow was restarted, the Eh and pH were monitored, and a sample was taken for Tc-99 analysis. This stopped-flow test was performed twice.

2.4 Grout Cylinder Leaching Experiment

Leaching of the simulated saltstone cylindrical specimens described in Section 2.1 was conducted following a modified ASTM C–1308 standard test method (ASTM International, 2001). Six specimens were used in the experiment—three were cured at room temperature and the other three at 60 °C [140 °F]. Each specimen, suspended by a Teflon monofilament from the cap of a 500-mL [30.5-in^3] polypropylene bottle (Figure 2-3), was immersed in 300 mL [18.3 in^3] of deionized water. The polypropylene bottles were kept in a constant temperature shaker water bath set at 25 °C [77 °F]. After each immersion period, each specimen was transferred to fresh water by moving the bottle cap (with the specimen attached) to a new bottle of deionized water. The specimens were transferred to fresh water every 24 hours for 6 consecutive days, then every 7 days for 6 consecutive weeks. This is different from the ASTM C–1308 standard procedure, which has replacement intervals of 2, 5, 17, and 24 hours, followed by replacement every 24 hours for another 9 days. The replacement interval used in this study is based on the recommendation of Ebert (2010), who stated the modified replacement interval will help distinguish between diffusion-controlled and dissolution-controlled release. Immediately after each specimen was moved to fresh water, 50-mL [3.1-in^3] samples were taken from the old leachates using a syringe with a 0.2-µm [7.9-µin] filter tip. Two 1-mL [0.06-in^3] aliquots were taken from each sample for Tc-99 activity

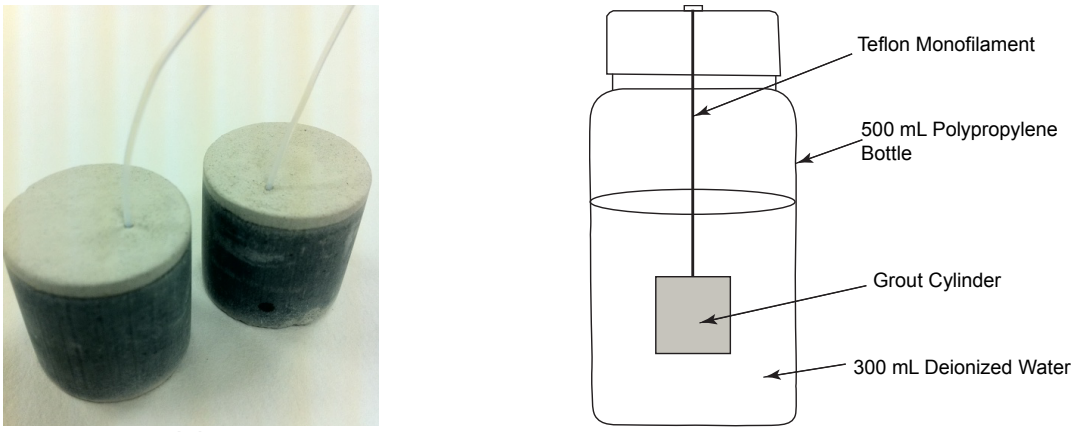

Figure 2-3. (a) Picture of 2.54-cm [1-in] Diameter by 2.54-cm [1-in] Length Simulated Saltstone Cylindrical Specimens and (b) Schematic Diagram of Cylindrical Specimen Immersed in Deionized Water Inside a Polypropylene Bottle

measurement, and the rest of each sample was split into two samples—one for metal analysis and the other for anion analysis.

2.5 Analytical and Characterization Methods

The Tc-99 activity of the aqueous samples was measured using a Packard 2505 TR/AB liquid scintillation counter and the Tc-activity of the solid samples was measured using a Ludlum Model 3030E alpha–beta counter. Aqueous concentrations of sodium, potassium, calcium, silicon, and aluminum were measured using a Spectro Analytical Instruments Model MFE-05 inductively coupled plasma–optical emission spectrometry unit (ICP–OES), whereas uranium, selenium, and iron aqueous concentrations were measured using a PerkinElmer® Elan® DRC II inductively coupled plasma–mass spectrometry system (ICP–MS). Magnesium concentrations were measured using ICP–MS or ICP–OES. Aqueous nitrate, nitrite, and sulfate concentrations were measured using a Dionex DX 500 ion chromatograph equipped with an Ion PAC AS14 analytical column.

The composition of the nonradioactive simulated saltstone was determined using energy dispersive x-ray spectroscopy (EDS), x-ray fluorescence (XRF) analysis, and x-ray diffraction (XRD) analysis. EDS and XRF analyses were used to determine the elemental composition of the simulated saltstone, whereas XRD analysis was used to determine the phase composition. EDS analysis was carried out using a Noran Voyager M3105 system, whereas XRF analysis was done using a ThermoARL AdvantXP+ x-ray fluorescence analyzer. XRD analysis was carried out with a Siemens D-500 x-ray diffractometer and a Kristalloflex 805 x-ray generator using Cu Kα radiation. Scanning electron microscopy (SEM) images of the surfaces of several nonradioactive simulated saltstone samples also were taken using a JEOL JSM-5800LV scanning electron microscope.

The surface area of the same material used in the column experiment was determined using a multipoint N_2-BET isotherm with a Coulter SA3100 surface area analyzer. In addition, its bulk density was measured using a pycnometer.

3 RESULTS

3.1 Grout Characteristics

The interior and sides of the uncontaminated simulated saltstone cylinder that was formed in the plastic mold are greenish gray in color (see Figure 3-1), with a white layer formed on the top surface [Figures 3-1(b) and 3-1(c)]. The white material is calcium carbonate, as evidenced by the XRD results described later and by a brisk effervescent reaction with dilute hydrochloric acid, which is characteristic of calcium carbonate (Deer, et al., 1966). Calcium carbonate formed on the grout surface that was exposed to the atmosphere while curing due to the reaction of the alkaline, calcium-rich cement pore fluid with atmospheric $CO_2(g)$.

Figure 3-2 is an SEM micrograph of small pieces of the nonradioactive simulated saltstone. Closeup SEM images were taken on two spots on the saltstone sample: one on the greenish–gray interior and the other on the white surface. The closeup micrographs are shown in Figures 3-3 and 3-4. SEM micrographs of a powdered piece of the greenish gray simulated saltstone also were taken and are shown in Figure 3-5. The elemental compositions of the simulated saltstone samples determined by EDS are shown in Figures 3-6 and 3-7 and in Table 3-1. Note that compositions determined by EDS are for specific areas on the sample, can vary significantly with sample location, and are not representative of the bulk sample composition.

Figure 3-8 shows the XRD patterns of the greenish gray and white simulated saltstone material, together with the diffraction patterns of reference solids, available in a computerized database, that best match the sample diffraction pattern. The dominant peaks in both samples correspond to quartz; to the calcium carbonate minerals aragonite, calcite, and vaterite; and to the aluminosilicate minerals sillimanite and mullite. The latter two minerals are high-temperature mineral phases that likely were present in the blast furnace slag or fly ash component of the grout mixture. The XRD data show that the white simulated saltstone material has more calcium carbonate minerals compared to the green material based on the higher calcium carbonate diffraction peaks in the former compared to the latter.

(a) **(b)** **(c)**

Figure 3-1. Photographs of (a) Uncontaminated Simulated Saltstone in Plastic Mold, (b) Top and Side of Simulated Saltstone Cylinder Showing White Layer Overlying Greenish Gray Grout, and (c) Partially Chipped Grout Cylinder Showing Greenish Gray Interior. The White Layer Evident in (b) and (c) Is Due to Calcium Carbonate.

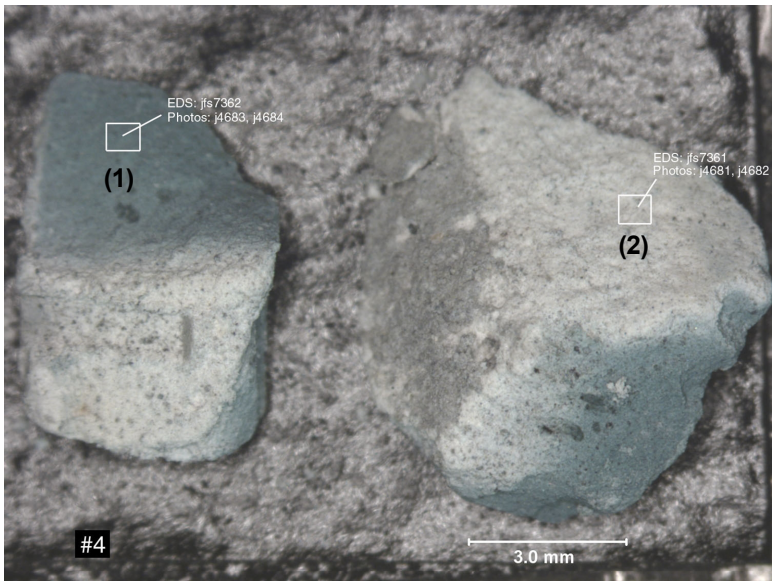

Figure 3-2. Scanning Electron Micrograph of Simulated Saltstone Sample. The Squares Indicate the Spots Where Closeup Images of the Material Were Taken and Elemental Analyses Were Done (See Figures 3-3, 3-4, and 3-6).

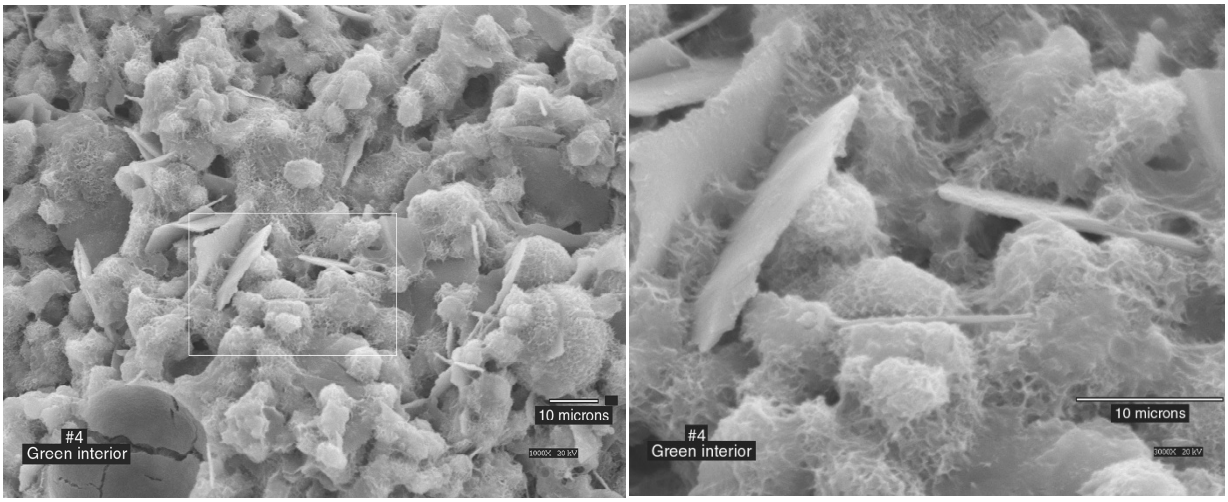

Figure 3-3. Closeup Scanning Electron Micrographs of the Greenish Gray Interior Surface of the Simulated Saltstone (Area 1 in Figure 3-2)

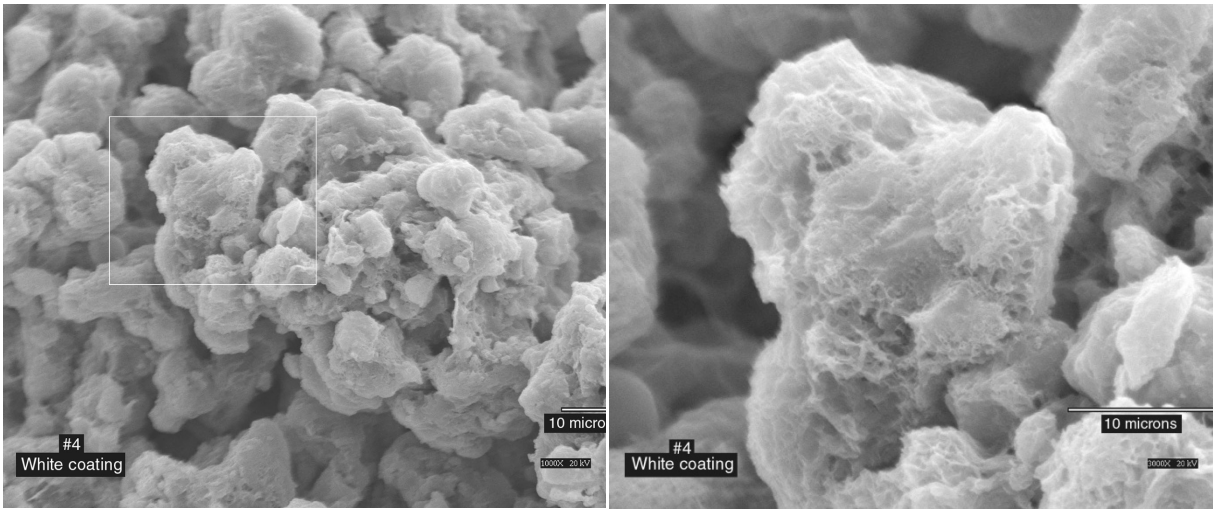

Figure 3-4. Closeup Scanning Electron Micrographs of the White Surface of the Simulated Saltstone (Area 2 in Figure 3-2)

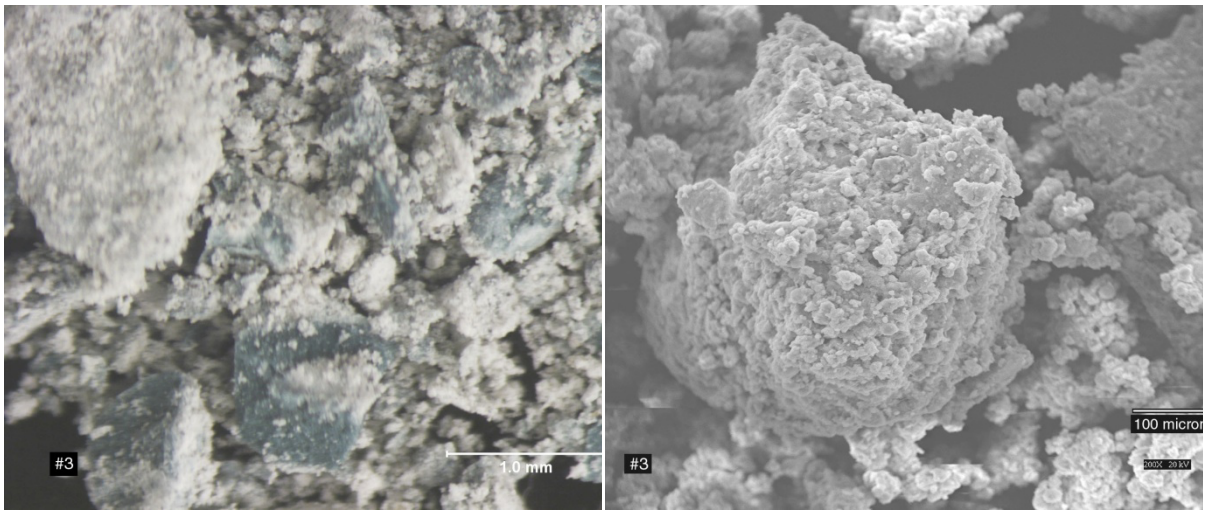

Figure 3-5. Scanning Electron Micrographs at Two Magnifications of a Powdered Piece of the Greenish Gray Simulated Saltstone

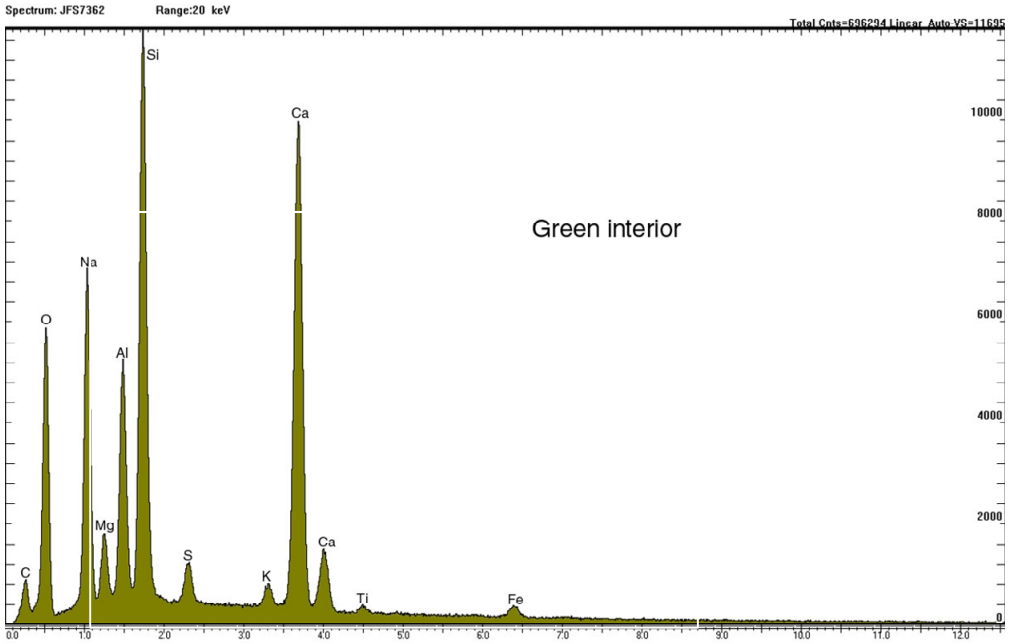

(a)

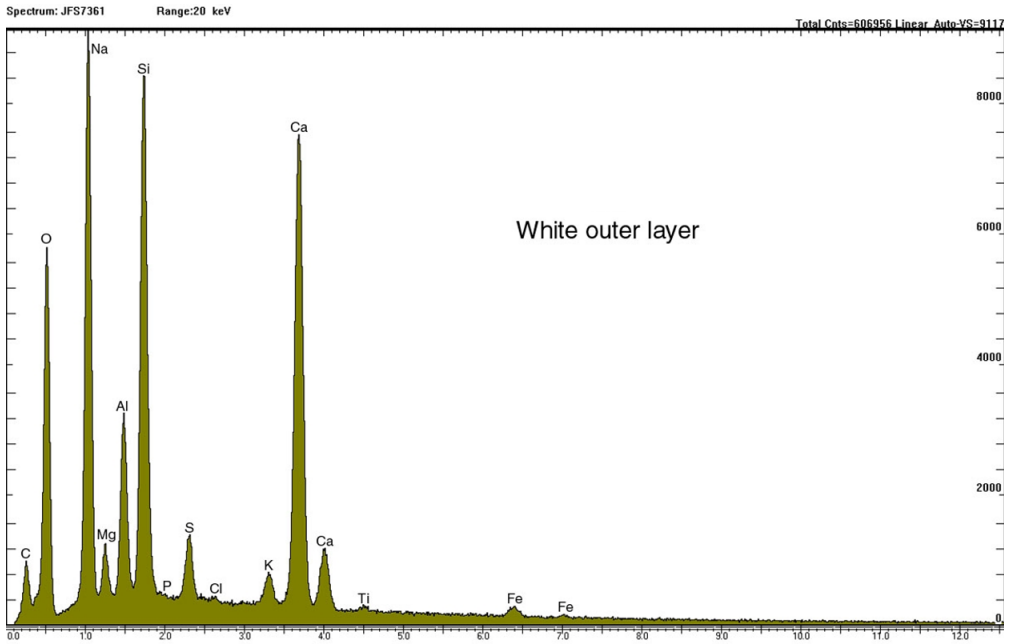

(b)

Figure 3-6. Elemental Spectra of the (a) Greenish Gray and (b) White Simulated Saltstone Material Determined Using Energy Dispersive X-ray Spectroscopy

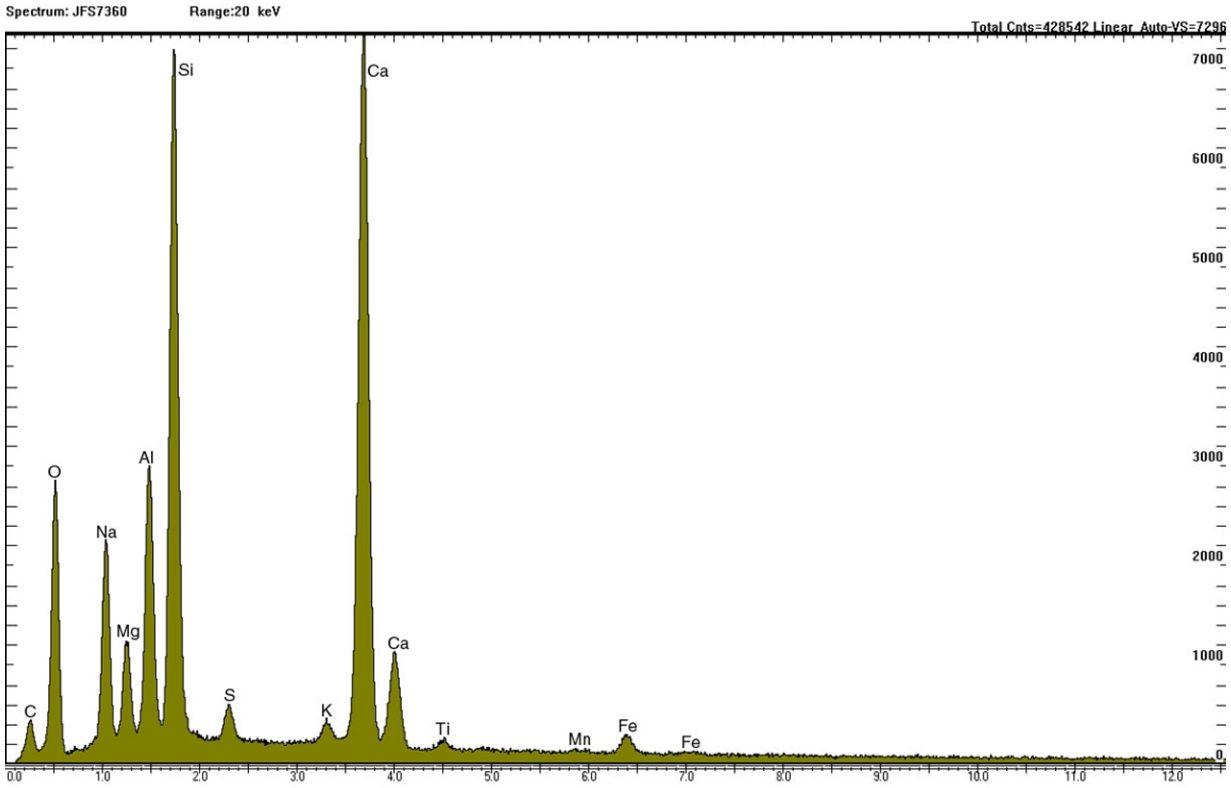

Figure 3-7. Elemental Spectrum of a Powdered Piece of the Greenish Gray Simulated Saltstone Determined Using Energy Dispersive X-ray Spectroscopy

Table 3-1. Elemental Composition (Atom %) of the Greenish Gray and White Simulated Saltstone Material

Element	Greenish Gray Material	Greenish Gray Powder	White Material
Na	24.8	14.9	36.6
Mg	3.67	4.56	2.92
Al	11.7	11.4	8.93
Si	27.7	28.8	23.0
P	—*	—*	0.17
S	2.76	2.08	3.54
Cl	—*	—*	0.24
K	0.93	0.71	1.21
Ca	27.0	35.2	22.2
Ti	0.34	0.59	0.4
Mn	—*	0.23	—*

*Below detection limit

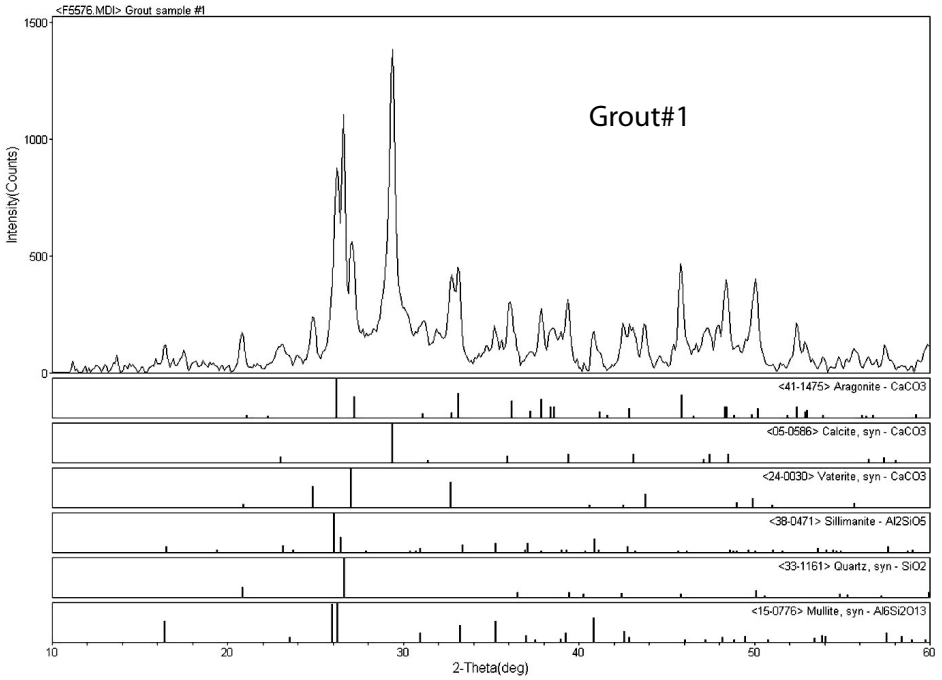

(a)

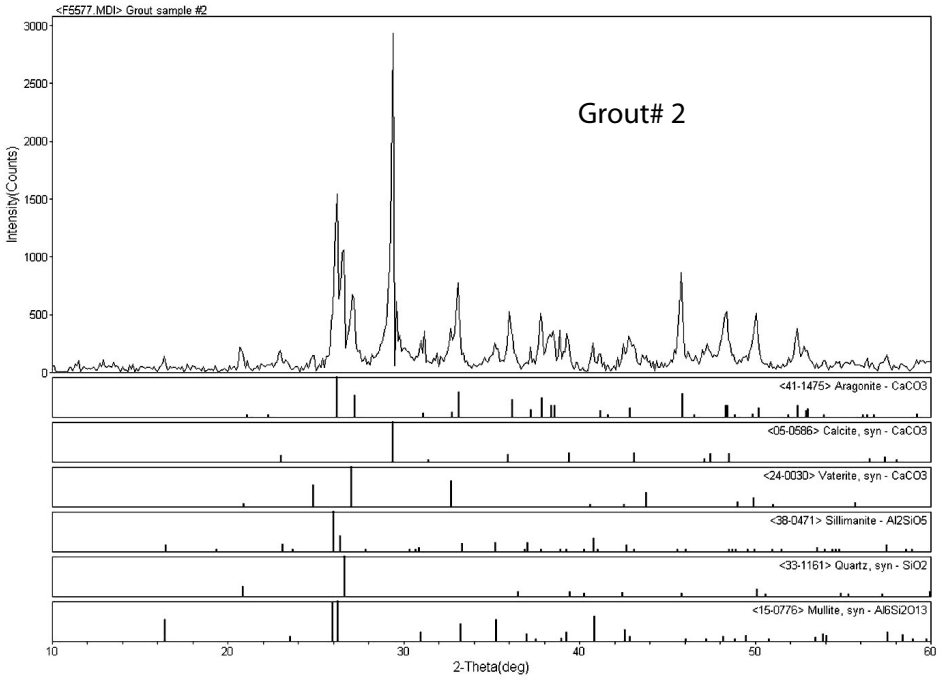

(b)

Figure 3-8. X-ray Diffraction Patterns of the (a) Greenish Gray and (b) White Simulated Saltstone Material. Also Shown Are the X-ray Diffraction Patterns of Reference Solids That Best Match the Sample Diffraction Pattern. Note the Difference in the Y-Axis Scales of (a) and (b).

Table 3-2 lists the chemical composition of the uncontaminated simulated saltstone determined using XRF analysis. Also shown are the chemical compositions of the blast furnace slag and fly ash materials that were used in preparing the simulated saltstone.

Table 3-3 lists the measured specific surface area, bulk density, and total mass of grout material loaded into Cells 1 and 2. The volume of grout material in the columns, calculated from the grout bulk density and total mass, also are listed in the table. Using the calculated column internal volume of 260 mL [15.9 in^3], the initial porosity of the grout material in Cells 1 and 2 is estimated to be 67 and 52 percent, respectively.

3.2 Column Experiment Results

The following sections describe the evolution of solution pH, Eh, aqueous concentrations, and contaminant release from the grout columns (Cells 1 and 2). During the initial stages of the experiment, gas bubbles were observed to form in the columns—more so in Cell 1 than in Cell 2—as the simulated SRS groundwater reacted with the reducing grout. The difference in degree of gas generation between Cells 1 and 2 could be due to the different slag components used. The gas bubbles migrated downstream from the column through the flow system and sometimes lingered inside the pH and redox microflow cells, which interfered with the microflow-through pH and redox measurements. Gas bubble formation abated after several pore volumes of simulated groundwater had reacted with the reducing grout. The gases are most likely $H_2(g)$ and $H_2S(g)$, based on the reducing character of the grout and the presence of sulfide in the blast furnace slag. The presence of $H_2S(g)$ also was indicated by a "rotten egg."

Table 3-2. Chemical Composition (Weight %) of Simulated Saltstone, Blast Furnace Slag, and Fly Ash*

Oxide Component	Simulated Saltstone†	Blast Furnace Slag‡	Fly Ash
SiO_2	30.03 ± 0.06	33.49 ± 0.23	55.64 ± 0.02
TiO_2	0.62 ± 0.00	0.50 ± 0.00	1.36 ± 0.00
Al_2O_3	11.49 ± 0.07	10.46 ± 0.05	23.94 ± 0.02
FeO*	1.56 ± 0.00	0.58 ± 0.00	3.67 ± 0.01
MnO	0.13 ± 0.00	0.32 ± 0.00	0.04 ± 0.00
MgO	4.03 ± 0.11	9.80 ± 0.05	1.85 ± 0.01
CaO	20.90 ± 0.47	40.06 ± 0.19	8.96 ± 0.02
Na_2O	4.91 ± 0.04	0.26 ± 0.01	0.24 ± 0.01
K_2O	0.48 ± 0.01	0.41 ± 0.00	0.93 ± 0.01
P_2O_5	0.09 ± 0.00	0.02 ± 0.00	0.10 ± 0.00
Sum	74.22 ± 0.55	95.88 ± 0.54	96.70 ± 0.01
Loss on Ignition (%)#	23.34 ± 0.58	0.86 ± 0.06	0.21 ± 0.07
SO3 ≥§	0.44 ± 0.05	0.34 ± 0.01	0.08 ± 0.01

*Measured using x-ray fluorescence analysis. Reported values are based on analysis of two samples.
†Sample taken from the interior portion of the uncontaminated simulated saltstone cylinder
‡LaFarge North America blast furnace slag
#Loss on ignition was determined by heating the sample at 900 °C [1,652 °F] for 16 hours.
§SO_3 values are reported as minimum values because sample preparation using a 1,000 °C [1,832 °F] muffle furnace causes unconstrained degassing.

Table 3-3. Characteristics of Crushed and Sieved Grout Material Loaded Into Column Experiment Cells 1 and 2		
	Cell 1	**Cell 2**
Density of grout material	2.47 g/cm^3 [1.43 oz/in^3]	1.92 g/cm^3 [1.11 oz/in^3]
Surface area	24.5 m^2/g [7,480 ft^2/oz]	32.9 m^2/g [10,000 ft^2/oz]
Total grout mass loaded into cell	209 g [7.37 oz]	242 g [8.54 oz]
Calculated volume of grout loaded into cell	85 mL [5.2 in^3]	126 mL [7.5 in^3]
Calculated porosity of grout material in cell	67%	52%

smell of some of the effluent solutions. The presence of reduced sulfur species, mainly as thiosulfate, also was observed from the ion chromatography analyses.

To facilitate the extrapolation of experimental data to other flow rates, the results are presented in terms of number of pore volume, instead of time. The number of pore volume was calculated from the equation

$$n_{pv} = \frac{f \cdot t}{V_c \cdot \phi} \tag{3-1}$$

where

n_{pv} = number of pore volume
f = flow rate (mL/min)
t = cumulative time (min)
V_c = flow cell internal volume (mL)
ϕ = effective porosity

As indicated in the preceding section, the flow cell internal volume is 260 mL [15.9 in^3] and the initial porosity of the grout material in Cells 1 and 2 is 67 and 52 percent, respectively. Thus, 1 pore volume (= $V_c \times \phi$) is equal to 174 and 135 mL [10.6 and 8.24 in^3], respectively, for Cells 1 and 2.

The use of Eq. (3-1) assumes the effective porosity is invariant with time. In calculating the pore volume of solution that flowed through the column, detailed accounting was made of the duration and flow rate when the HPLC pump was on. This procedure is important because the solution flow frequently had to be interrupted (e.g., to take samples, replace Tedlar bags, or fix leaks in the pH or Eh microflow cells) and the flow rate during sampling of Cell 2 was higher {0.5 mL/min [0.031 in^3/min]} than the normal flow rate of 0.066 mL/min [0.0040 in^3/min].[2]

[2]The higher flow rate during Cell 2 sampling means a shorter residence time in the column of the ~50 mL [3.1 in^3] sample, which is 37 percent of the column pore volume, and less reaction of the solution with the grout. Less reaction should have resulted in a consistently lower concentration of all aqueous species in the Cell 2 test compared to the Cell 1 test, which was not observed in the experimental data. Thus, the higher flow rate during sampling appears not to have unduly affected the Cell 2 experimental results.

Data on contaminant (e.g., technetium, nitrate, nitrite, selenium) release also are presented in terms of cumulative amount or fraction leached from the simulated saltstone. These quantities are calculated using the following equations

$$n_{cum,N}(t) = \sum_{i=1}^{t} (\Delta n_{pv,i} \cdot V_c \cdot \phi \cdot M_{s,N,i} / 1000) \quad (3\text{-}2)$$

$$F_{cum,N}(t) = \frac{n_{cum,N}(t)}{n_{t,N}} \quad (3\text{-}3)$$

where

$n_{cum,N}(t)$ = cumulative number of moles of contaminant (N) leached from the grout at time t

$M_{s,\mathrm{N,i}}$ = measured contaminant molarity (mol/L) in the aqueous sample taken at time t_i

$n_{t,N}$ = total moles of contaminant initially in the grout column

$F_{cum,N}(\mathrm{t})$ = cumulative mole fraction of contaminant leached from the grout column at time t

$\Delta n_{pv,I}$ = pore volume of solution that exited the column between time t_i and t_{i-1}

The initial amount ($n_{t,N}$) of technetium in Cells 1 and 2 is equal to 3.92×10^{-6} and 4.49×10^{-6} moles, respectively, based on the Tc-99 activity in the technetium spike and the mass of grout material in the columns. The initial amounts of nitrate in Cells 1 and 2 are 0.171 and 0.194 moles, respectively, and those of nitrite are 8.55×10^{-3} and 9.70×10^{-3} moles, respectively, based on the nitrate and nitrite concentration in the DDA simulant solution and the amount of grout material in the columns. The initial amounts of uranium and selenium in Cell 2 are 6.56×10^{-4} and 2.22×10^{-4} moles, respectively, based on the uranium and selenium mass added to the grout mix and the grout mass loaded in Cell 2.

3.2.1 Cell 1 Effluent Solution Chemistry

pH

Figure 3-9 shows as a function of pore volume the Cell 1 solution pH measured using the Orion ROSS combination pH electrode. The pH initially was 12.9, then fell continuously for about 12 pore volumes to a value of 11.8. After 14 pore volumes, the pH decreased much more slowly, reaching only 11.1 after 134 pore volumes. pH buffering at 12.5, which is expected in a grout that has significant portlandite, was not observed. Portlandite likely did not form in significant amounts, because the grout dry mix only had 10 wt% Portland cement and calcium hydroxide would have reacted with the silica and alumina in fly ash and blast furnace slag to form C-S-H and strätlingite (Pabalan, et al., 2009). Only the offline Orion pH electrode measurements are plotted because the inline microflow-through pH electrode gave erratic results due to the gas bubbles that formed from the reaction of the simulated SRS groundwater with the reducing grout and got trapped in the microflow-through pH cell cavity.

Redox Potential

The redox potentials in Cell 1, given in terms of Eh, are plotted as a function of pore volume in Figure 3-9. The Eh values were derived from the redox potentials measured with the

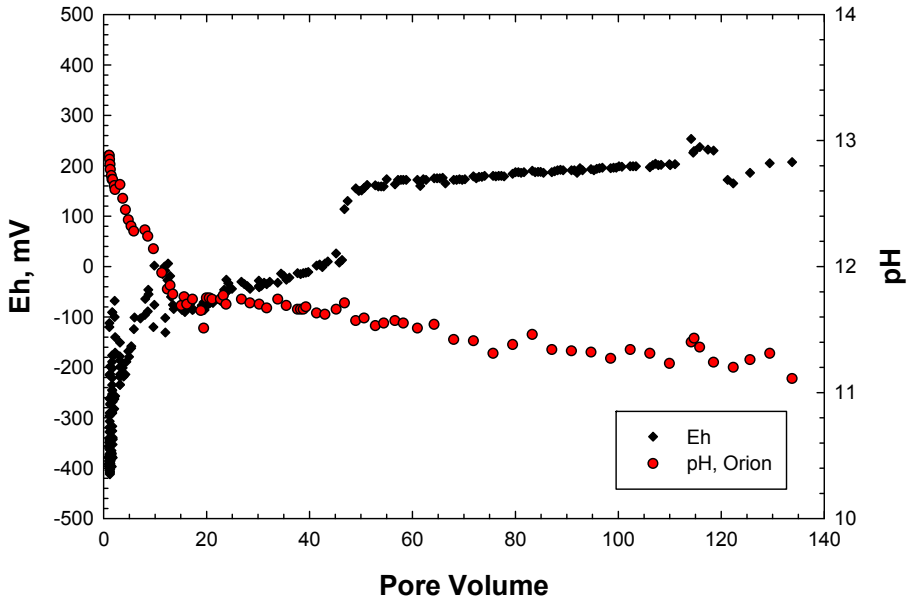

Figure 3-9. Cell 1 Measured pH and Eh as a Function of Number of Pore Volume

microflow-through redox probe, which has a Ag/AgCl internal reference electrode, by adding 200 mV. The system initially was very reducing, with a lowest Eh reading of −404 mV, but relatively quickly increased to higher redox potentials. There was considerable scatter in Eh values, likely due to interference by gas bubbles, but the redox measurements became more stable after about 13 pore volumes as the gas generation abated. The Eh gradually increased from pore volumes 12 to 44, then suddenly increased by 120 mV at 46 pore volumes. Further Eh increases were more gradual except during the period from 110 to 129 pore volumes. After 110 pore volumes, the HPLC pump required repair and the experiment was on hold for 4 weeks. There was significant variation in Eh between 110 and 129 pore volumes after the experiment was restarted as the system readjusted toward its previous steady-state condition.

Aqueous Species Concentrations

The measured aqueous concentrations of Cell 1 effluent solution are plotted in Figures 3-10 and 3-11. The results indicate that with the exception of calcium, the aqueous species concentrations decreased significantly through the first 14 pore volumes then subsequently changed much more slowly or remained constant. The calcium concentration was relatively constant during the first 8 pore volumes, increased sixfold during the next 12 pore volumes, then gradually declined after that. Potassium, aluminum, sulfate, nitrate, and nitrite concentrations gradually declined after 14 pore volumes, whereas silicon concentration showed a slightly increasing trend. Sodium concentration was relatively constant after about 30 pore volumes. The magnesium and iron data are more limited,[3] but their concentrations were relatively constant after 14 pore volumes. The significant change in the aqueous concentrations

[3]Magnesium and iron concentrations plotted in Figure 3-10 were measured using ICP–MS. Later samples were analyzed for magnesium and iron concentrations using ICP–OES, which has higher detection limits than ICP–MS. The measured magnesium and iron concentrations of the later samples were below the detection limit of ICP–OES and, therefore, were not plotted in Figure 3-10.

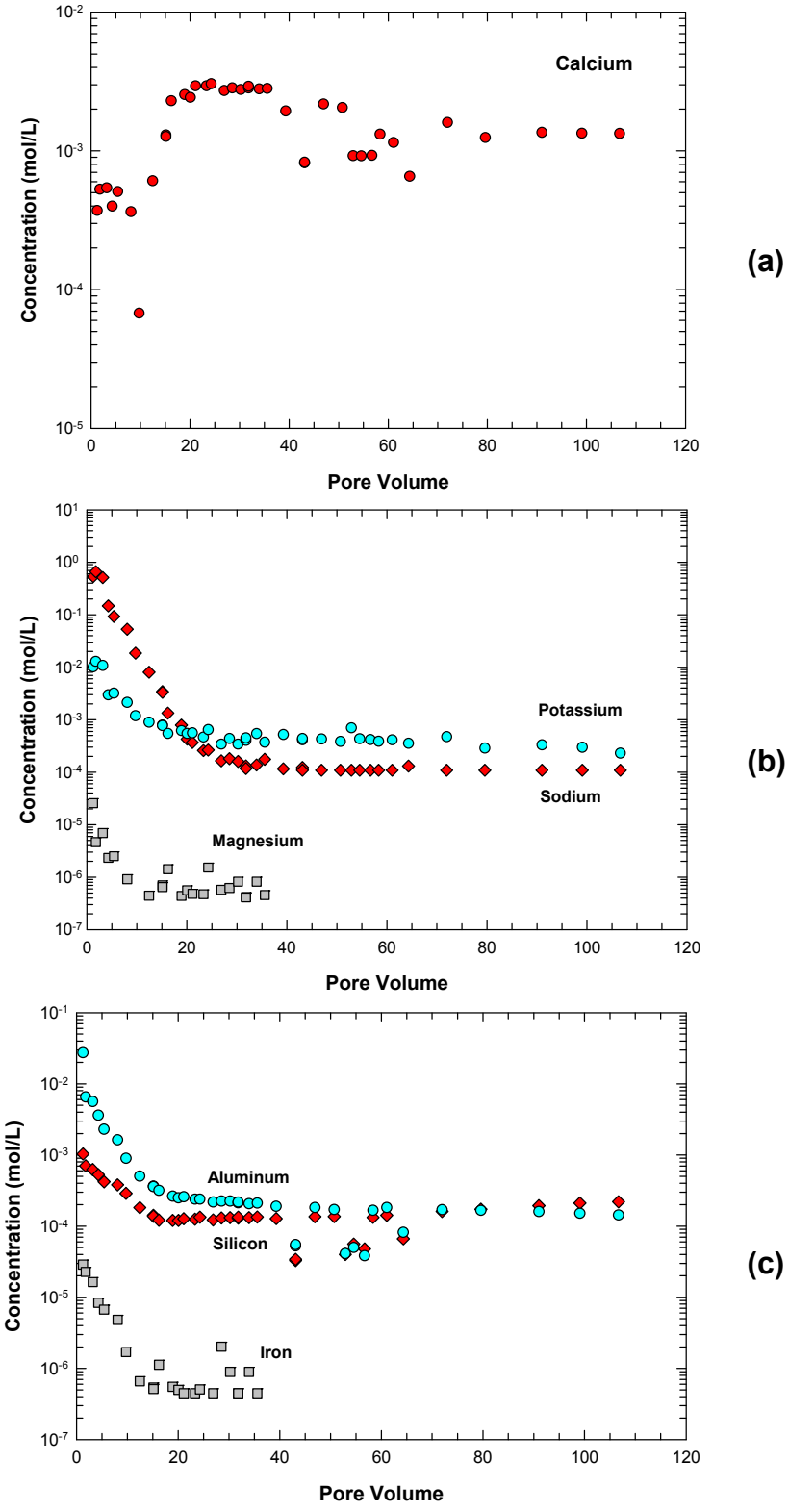

Figure 3-10. Measured Concentrations of (a) Calcium; (b) Sodium, Potassium, and Magnesium; and (c) Aluminum, Silicon, and Iron in Cell 1 Effluent Solution as a Function of Number of Pore Volume

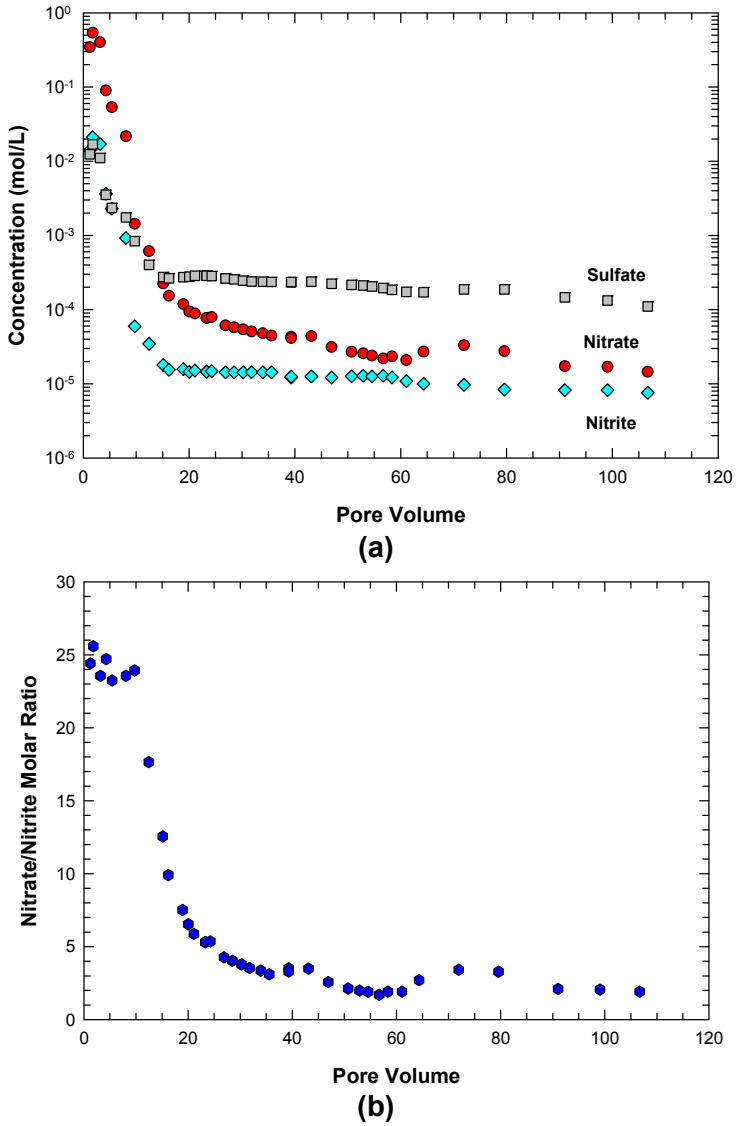

Figure 3-11. (a) Measured Nitrate, Nitrite, and Sulfate Concentrations and (b) Calculated Nitrate-to-Nitrite Molar Ratio in Cell 1 Effluent Solution as a Function of Number of Pore Volume

during the first 14 pore volumes is likely due to advective release of aqueous species initially dissolved in the grout pore solution. The change in aqueous concentration after 14 pore volumes became more gradual as the concentration became increasingly controlled by grout dissolution.

The nitrate/nitrite molar ratio, shown in Figure 3-11(b), initially was high, between 23 and 26 through the first 10 pore volumes, then decreased exponentially after that. The initially high nitrate/nitrite ratio corresponds to that of the DDA simulant solution (≈25, see Table 2-1) that was used to prepare the simulated saltstone. After 10 pore volumes, the ratio no longer was controlled by the initial amount of nitrate and nitrite in the DDA simulant solution and decreased exponentially.

Technetium Release

Figure 3-12 plots the calculated cumulative mass of Tc-99 leached from the Cell 1 grout and the measured technetium concentration in Cell 1 effluent solution as a function of pore volume. The data show that technetium released from the simulated saltstone grout increased sharply during the first 10 pore volumes. This initial increase in technetium release approximately corresponds to the observed early Eh increase and pH decrease shown in Figure 3-9 and is likely due to the advective release of technetium initially dissolved in the grout pore solution, as discussed in a following paragraph. After the initial 10 pore volumes, Tc-99 was relatively retained by the saltstone simulant before significant release initiates at 52 pore volumes. Acknowledging that the spatial and temporal variation in chemical conditions along the column flow path is complex, it appears that the Tc-99 release corresponded to the step increase in Eh that occurred at

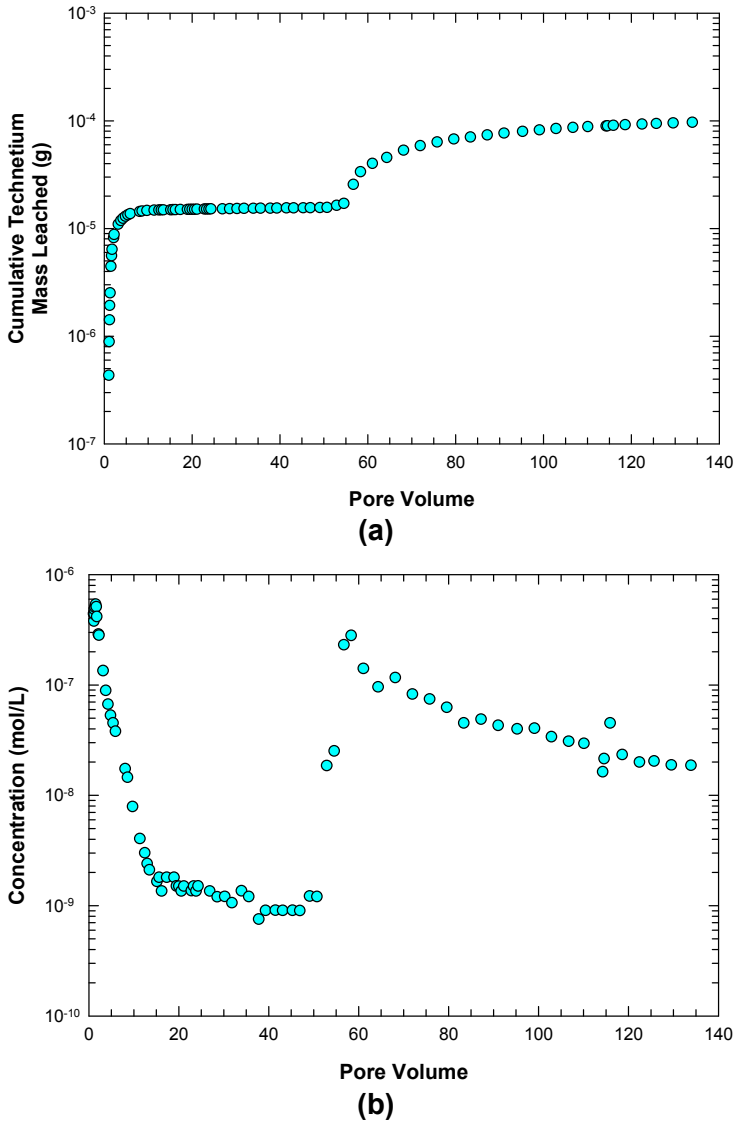

Figure 3-12. (a) Calculated Cumulative Mass of Tc-99 Leached From the Simulated Saltstone and (b) Measured Technetium Concentration in Leachant Solution as a Function of Number of Pore Volume. The Initial Technetium Mass in the Cell 1 Grout Was 3.88×10^{-4} g [1.37×10^{-5} oz].

46 pore volumes and is likely a result of oxidative dissolution of Tc(IV) sulfide and/or oxide phases in the reducing grout. There was a time lag between Eh increase and technetium release, possibly due to slow oxidation of technetium at depth within particles, which in turn is likely controlled by oxygen diffusion into the particles.

The cumulative fraction of technetium leached from the Cell 1 grout column as a function of pore volume is compared with that of nitrate and nitrite in Figure 3-13(a). The curves for technetium, nitrate, and nitrite have similar shapes that indicate an exponential increase in fraction leached from the column during the first several pore volumes, followed by relatively constant values until 52 pore volumes, with the cumulative fractions of nitrate and nitrate

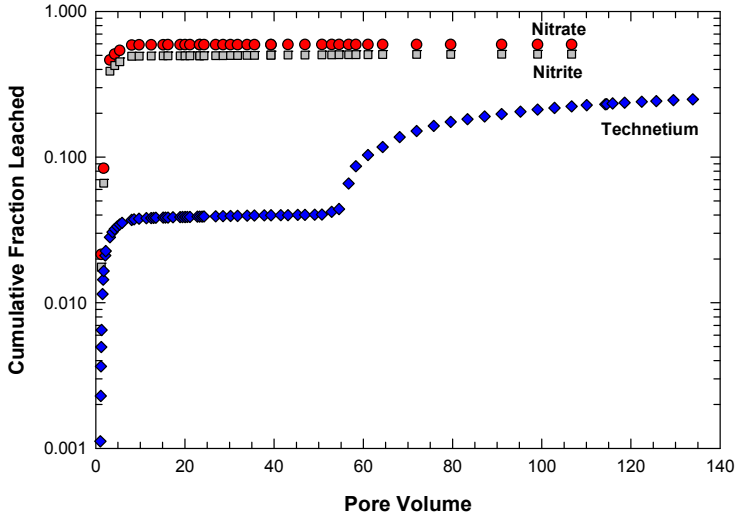

(a)

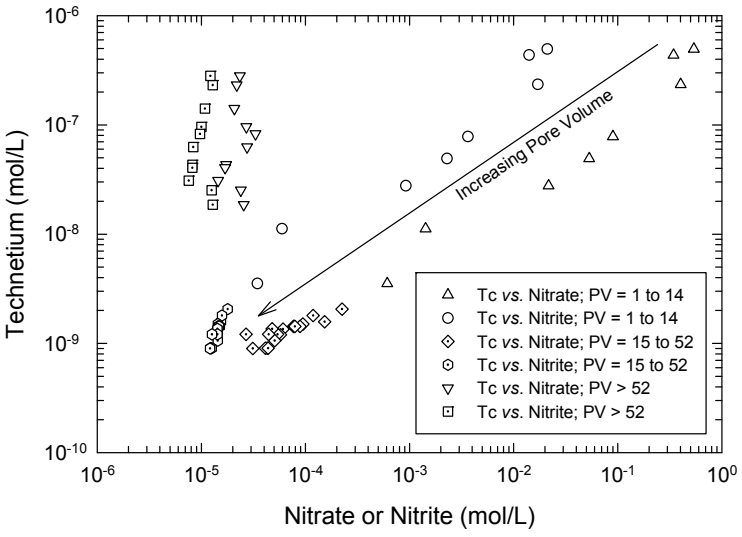

(b)

Figure 3-13. (a) Calculated Cumulative Fraction of Nitrate, Nitrite, and Technetium Leached From Cell 1 Simulated Saltstone as a Function of Number of Pore Volume. (b) Technetium Versus Nitrate or Nitrite Concentration in Cell 1 Effluent Solution. In (b), Different Symbols Represent Values at Different Ranges of Pore Volume.

leached from the column 10 times greater than that of technetium. After 52 pore volumes, the trends in nitrate and nitrite cumulative fraction release remained the same, but technetium release significantly increased. The technetium cumulative fraction leached was 0.04 at 52 pore volumes and 0.25 at 134 pore volumes.

Figure 3-13(b) plots the technetium concentration in Cell 1 effluent solution versus that of nitrate or nitrite. During the first 14 pore volumes, technetium concentration quickly decreased with increasing pore volume approximately linearly with nitrate and nitrite concentration. This trend is likely due to the advective release of technetium, nitrate, and nitrite initially dissolved in the grout pore water and the increasing dilution of aqueous concentrations by infiltrating simulated SRS groundwater. Blast furnace slag hydration is relatively slow, and it is possible not all of the Tc(VII) in the Tc-99 spike was reduced to the low solubility Tc(IV) oxidation state in the cured grout. In addition, partial reoxidation of Tc(IV) in the grout could have occurred during the crushing and sieving of the grout material. The technetium that was released early likely represents the unreduced or reoxidized technetium. The decrease in technetium, nitrate, and nitrite concentrations was more gradual at 15 to 52 pore volumes (also shown in Figures 3-11 and 3-12) as the initially dissolved species were consumed and the aqueous concentrations started to be controlled by grout leaching. The technetium, nitrate, and nitrite concentrations at >52 pore volumes represent leaching from the simulated saltstone material, approximately coincident with an increase in system Eh. Technetium release at these higher pore volumes is likely controlled by the oxidation and dissolution of a Tc(IV) phase.

Langton's (1987) data on technetium and nitrate leached from a saltstone formulation composed of Portland cement, blast furnace slag, and fly ash versus time are plotted in Figure 3-14. For comparison, data from this study also are plotted in the figure. Note that Langton's (1987) study used monolithic specimens that were immersed in test solutions, in contrast to the column experiment in this study using crushed and sieved material. As shown in the figure, both studies show similar trends in nitrate leached fraction versus time. The trends in technetium leached fraction versus time also are similar until about 95 days (corresponding to

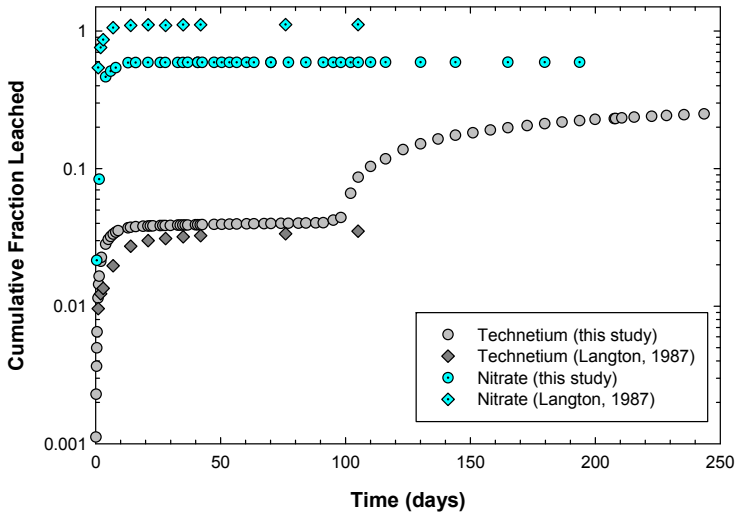

Figure 3-14. Data From This Study and Langton (1987) on Cumulative Fraction of Nitrate and Technetium Leached From Simulated Saltstone Versus Time. Langton (1987) Used a Monolithic Saltstone Specimen, Whereas Crushed and Sieved Material Was Used in This Study. Langton (1987) Explained the Greater Than 1.0 Values of Cumulative Fraction of Nitrate Leached as an Artifact of Nitrate in the Specimen Pore Solutions.

53 pore volumes in this study). Beyond 95 days, data from this study show a significant increase in technetium release, whereas Langton (1987) did not observe an increase in technetium release. The monolithic test specimen Langton (1987) used likely precluded any significant oxidation of the reducing grout and prevented technetium release within the timeframe of the experiment.

Posttest Technetium Concentration in the Grout Column

Figure 3-15 shows the measured technetium mass that was leached from the 0.25-g [0.0088-oz] samples of Cell 1 grout extruded from the flow cell. The values of technetium mass leached from the three samples taken from each column section have relative standard deviations ≤8 percent, indicating the technetium is relatively homogeneously distributed radially in the grout column. Lengthwise along the column, the data indicate that technetium depletion of the grout is greatest near the column inlet and decreases toward the column outlet. Also shown in the figure is the technetium mass leached from the unused grout material. This value {4.57×10^{-7} g [1.61×10^{-8} oz]} is a measure of the technetium mass initially present in the as-prepared grout material.[4] The data in Figure 3-15 indicate that the fraction of technetium leached from the Cell 1 grout decreased from ~0.64 near the column inlet to ~0.46 near the column outlet. These values are higher than the 0.25 value of the cumulative fraction of technetium leached calculated using Eq. (3-3) and the Cell 1 grout column data [Figure 3-13(a)]. The lower value is probably due to the periodic sampling of effluent solutions, which may have

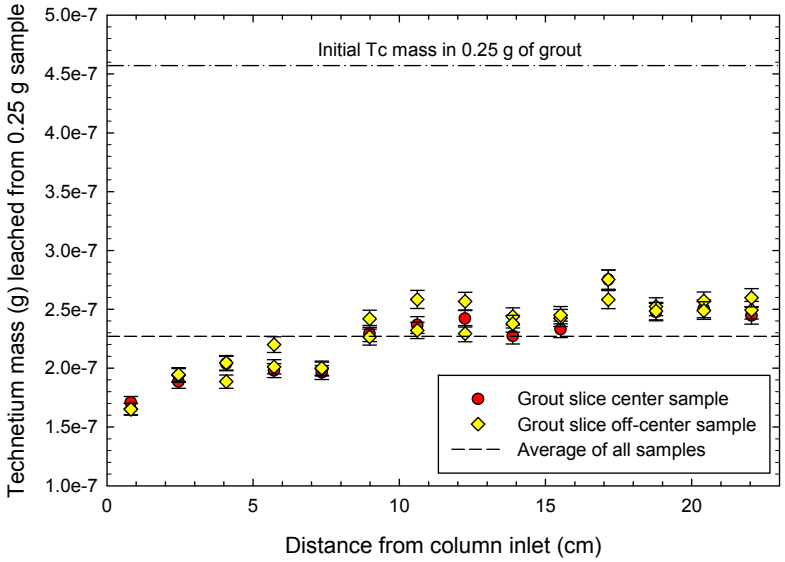

Figure 3-15. Technetium Mass Leached From 0.25-g [0.0088-oz] Samples of Cell 1 Simulated Saltstone Grout With 50 Volume Percent HNO_3 Solution. The Measured Initial Technetium Mass in a 0.25-g [0.0088-oz] Grout Sample Is 4.57×10^{-7} g [1.61×10^{-8} oz] and the Average Technetium Mass Leached From All the Samples Is 2.27×10^{-7} g [8.01×10^{-9} oz], Which Indicates an Average Technetium Leached Fraction of 0.50.

[4]The data plotted in Figure 3-15 are 5 percent higher than the measured values to account for the technetium that was not leached by the HNO_3 solution. The results of technetium measurements described in Section 2.3 of residual SSG solids and unleached grout material indicate that the 50 percent HNO_3 solution leached only 95 percent of the technetium in the grout. The Tc-99 activity of the residual SSG solids measured with the Ludlum Model 3030E alpha–beta counter was 17±1 counts per minute, whereas that of the unreacted grout samples was 330±12 counts per minute. The counting efficiency of the Ludlum instrument was 5 percent.

missed short periods of high technetium fractional release, such as those that occurred during the onset of the experiment or following the Eh transition. Notwithstanding the differences in the calculated technetium leached fraction, the data indicate that much of the technetium originally present in the column remained in a reduced, low solubility phase. This is consistent with a mass balance analysis comparing the amount of dissolved O_2 that has flowed through the column with that needed to consume the reducing capacity of the grout in the column.[5] The analysis indicates that much of the reducing grout in Cells 1 and 2 remained unoxidized.

The measured technetium mass leached from 0.25-g [0.0088-oz] samples of unused grout is 4.57×10^{-7} g [1.61×10^{-8} oz]. For comparison, the technetium mass in 0.25 g [0.0088 oz] of grout calculated from the mass of Tc-99 spike added to the Cell 1 grout is 4.64×10^{-7} g [1.64×10^{-8} oz]. The two values are in very good agreement.

3.2.2 Cell 2 Effluent Solution Chemistry

pH

Figure 3-16 shows, as a function of pore volume, the Cell 2 solution pH measured using the Lazar microflow pH electrode and the Orion ROSS combination pH electrode. In contrast to the Cell 1 data, the pHs measured with the Lazar and Orion pH electrodes are in good agreement through the first 83 pore volumes, probably because less gas was formed during the Cell 2 column experiment. The pH initially was 12.9, similar to the initial pH in Cell 1, then fell continuously for about 16 pore volumes to a value of 11.5. Similar to the Cell 1 results, no pH buffering at 12.5 was observed, indicating the grout had no significant portlandite to buffer the pH at that value. After 18 pore volumes, the pH remained relatively stable, varying between 11.32 and 11.48 up to 83 pore volumes, with an average value of 11.40 ± 0.05. The pHs measured using the Lazar electrode started to diverge from those measured using the Orion electrode after 83 pore volumes, with the former averaging 11.28 ± 0.04 and the latter averaging 11.45 ± 0.03. The divergence in the two sets of measurements is possibly due to a drift in the Lazar pH electrode, which has not been recalibrated since the start of the experiment.

Redox Potential

The Eh in Cell 2 is plotted as a function of pore volume in Figure 3-16. As in Cell 1, the system initially was very reducing, with a lowest Eh reading of −453 mV, but relatively quickly increased to higher redox potentials. There was less scatter in initial Eh values compared to Cell 1. The Eh quickly increased from −453 mV at 6 pore volumes to +180 mV at 22 pore volumes. Further

[5]Roberts and Kaplan (2009) measured a reduction capacity for simulated saltstone of 0.820 meq e^-/g. Based on this value and the grout mass loaded in the flow cells (Table 3-3), the reduction capacities of the grout in Cells 1 and 2 are 171 and 198 meq e^-, respectively. Based on an O_2 aqueous solubility of 2.65×10^{-4} molar (Kaplan and Hang, 2007), which is equivalent to 1.06 meq e^-/L, the 134 and 132 pore volumes of solution {equivalent to 23.3 and 17.8 L [6.16 and 4.70 gal]} that have flowed through Cells 1 and 2, respectively, would have consumed 25 and 19 meq e^- of reduction capacity, which represents 15 and 10 percent of the total reduction capacity of the grout in Cells 1 and 2, respectively. Alternative estimates of Cells 1 and 2 grout-reducing capacity are 43 and 50 meq e^-, respectively, based on the presence of 25 weight percent blast furnace slag in the grout and a measured slag-reducing capacity equal to 819 meq e^-/g (Roberts and Kaplan, 2009). Using these reduction capacity values, the 134 and 132 pore volumes of solution that have flowed through Cells 1 and 2 would have consumed 58 and 48 percent, respectively, of the grout-reducing capacity in Cells 1 and 2. These estimates of grout-reducing capacity consumed by dissolved O_2 do not account for the grout that was oxidized during preparation of the crushed and sieved material and assume that 100 percent of the dissolved O_2 in the solution that flowed through Cells 1 and 2 reacts with the grout.

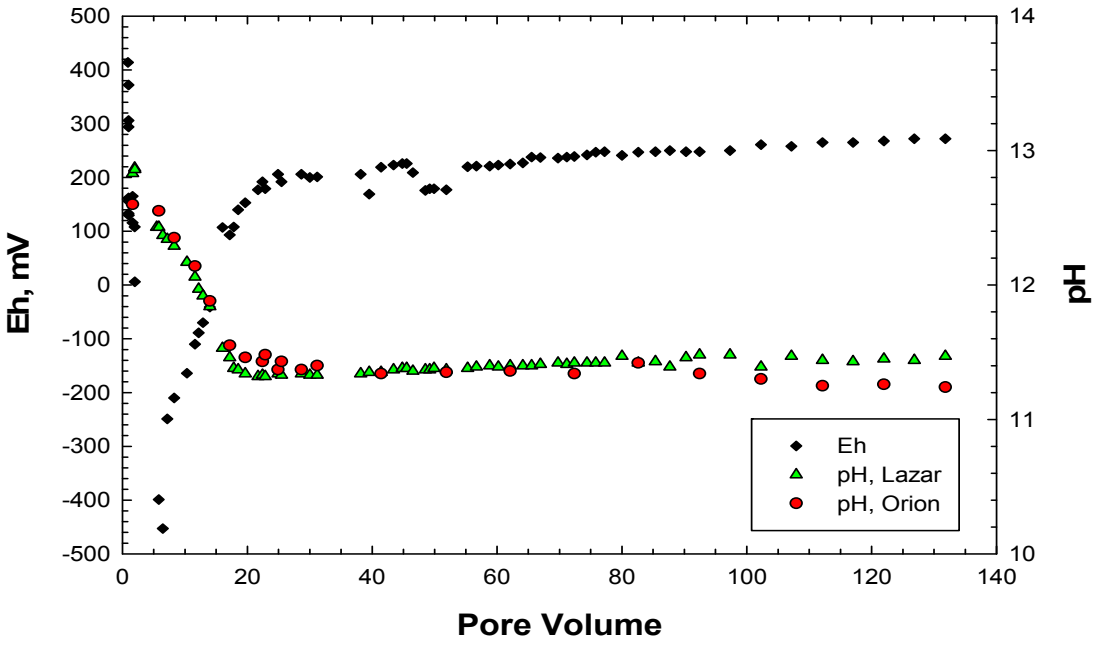

Figure 3-16: Measured Concentrations of (a) Calcium; (b) Sodium, Potassium, and Magnesium; and (c) Aluminum, Silicon, Selenium, and Iron in Cell 2 Effluent Solution as a Function of Number of Pore Volume

Eh increases were more gradual, and no sudden Eh increase as in Cell 1 was observed. An Eh of 272 mV was measured at 132 pore volumes.

Aqueous Species Concentrations

The measured aqueous concentrations of Cell 2 effluent solution for 132 pore volumes are plotted in Figures 3-17 and 3-18. The aqueous concentrations of sodium, potassium, selenium, and sulfate decreased significantly through the first 20 pore volumes, then subsequently decreased more slowly. Calcium concentration decreased during the first 6 pore volumes, increased significantly through the next 20 pore volumes, then was relatively constant afterwards. Silicon concentration initially increased, then decreased significantly up to 20 pore volumes, and then showed a slightly increasing trend afterwards. Aluminum concentration showed a similar initial increase, followed by a significant decrease up to 20 pore volumes, then a gradual decrease at higher pore volumes. Iron, nitrate, and nitrite concentrations quickly decreased below the reporting limit of the analytical method. The nitrate/nitrite molar ratio, shown in Figure 3-18(b), initially was high (25.7) and approximately equal to the DDA simulant solution nitrate/nitrite ratio (≈25, see Table 2-1), then decreased exponentially with increasing pore volume. Nitrate/nitrite molar ratios after 31 pore volumes are not plotted, because both nitrate and nitrite concentrations were below the reporting limit of the ion chromatography analytical method.

Technetium, Uranium, and Selenium Release

Figure 3-19 plots the calculated cumulative fractions of technetium and selenium leached from the Cell 2 grout column as a function of pore volume. Included in the figure are calculated nitrate and nitrite cumulative fractions leached. Uranium values are not plotted, because the measured uranium concentrations were mostly below the ICP–MS detection limit (0.002 ppm), indicating uranium was retained in the simulated saltstone grout.

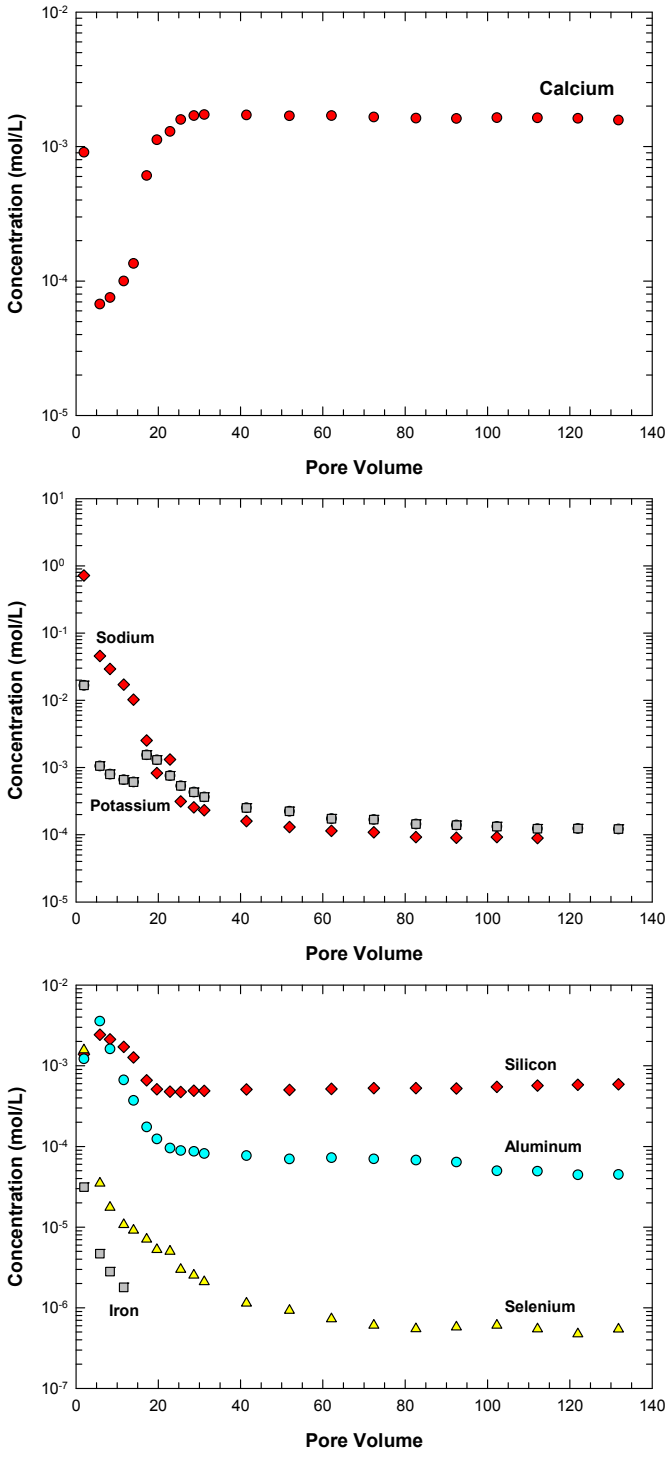

Figure 3-17. Measured Concentrations of (a) Calcium; (b) Sodium and Potassium; and (c) Silicon, Aluminum, Selenium, and Iron in Cell 2 Effluent Solution as a Function of Number of Pore Volumes

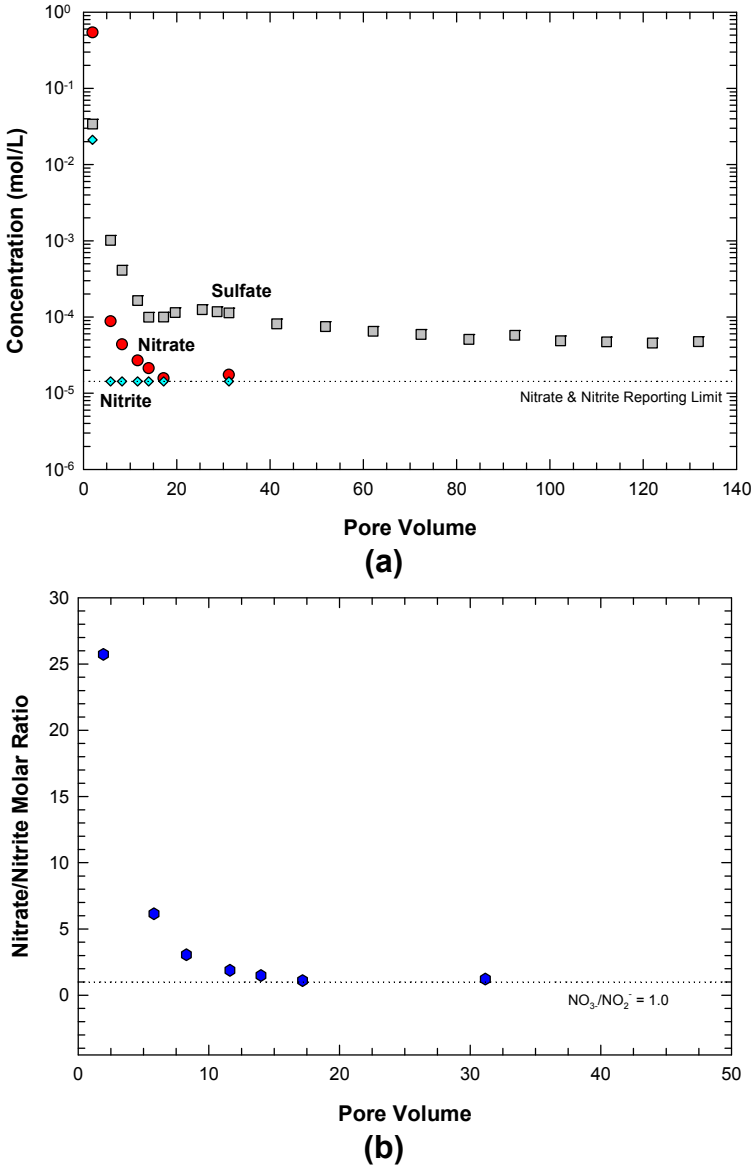

Figure 3-18. (a) Measured Nitrate, Nitrite, and Sulfate Concentrations and (b) Calculated Nitrate-to-Nitrite Molar Ratio in Cell 2 Effluent Solution as a Function of Number of Pore Volumes. After 31 Pore Volumes, the Nitrate and Nitrite Concentrations Are Below the Ion Chromatography Reporting Limit (0.2 ppm Nitrogen) and Are Not Plotted.

The cumulative fractions of technetium, selenium, nitrate, and nitrite leached at 2 pore volumes were 0.088, 0.63, 0.73, and 0.57, respectively. Because no samples before 2 pore volumes were taken, the initial rapid rise in technetium, nitrate, and nitrite values shown by Cell 1 data was not observed in Cell 2 data. Nitrate and nitrite leaching essentially were negligible after 20 pore volumes as their aqueous concentrations were below the reporting limit of the analytical method. In contrast, selenium was continually released, reaching a cumulative fraction leached of 0.97 at 132 pore volumes. The selenium data are consistent with those of Gerdes, et al. (2007), who stated that slag-bearing saltstone does not retain much of the selenium initially in the grout and that essentially all of the selenium is released during leaching.

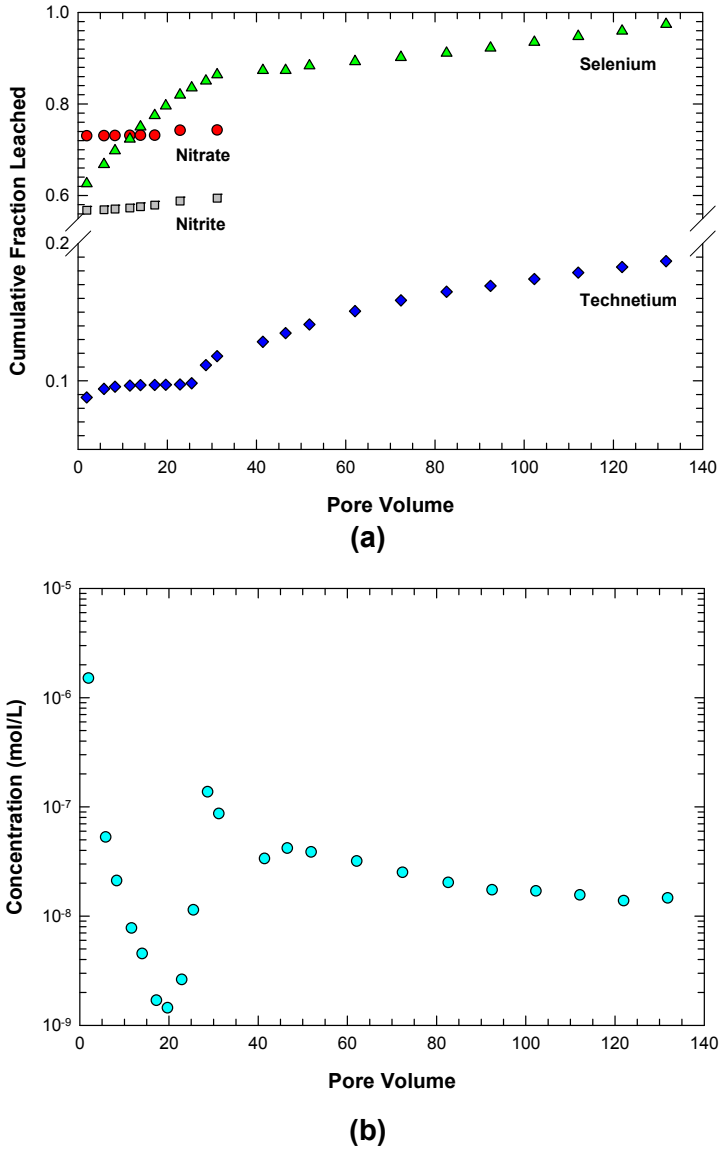

Figure 3-19. (a) Calculated Cumulative Fraction of Technetium, Selenium, Nitrate, and Nitrite Leached From Cell 2 Simulated Saltstone and (b) Measured Technetium Concentration in Leachant Solution as a Function of Number of Pore Volume

The technetium cumulative fraction leached was relatively constant at ~0.1 up to ~26 pore volumes, ~2.5 times the Cell 1 values between 10 and 52 pore volumes. At >26 pore volumes, the technetium cumulative fraction leached increased with increasing pore volume. The technetium cumulative fraction leached at 132 pore volumes was 0.19, which is lower than the 0.25 value attained in the Cell 1 test at 134 pore volumes [Figure 3-13(a)].

Results of Stopped-Flow Test

As described in Section 2.3, flow to Cell 2 was interrupted twice during the later part of the experiment to let the solution react with the reducing grout for a longer time period. Figure 3-20 shows the measured Cell 2 Eh and pH after the flow was restarted. The Eh initially was ≥360 mV and the pH initially ≤9.3 after the flow was restarted, which reflect the Eh and pH of the

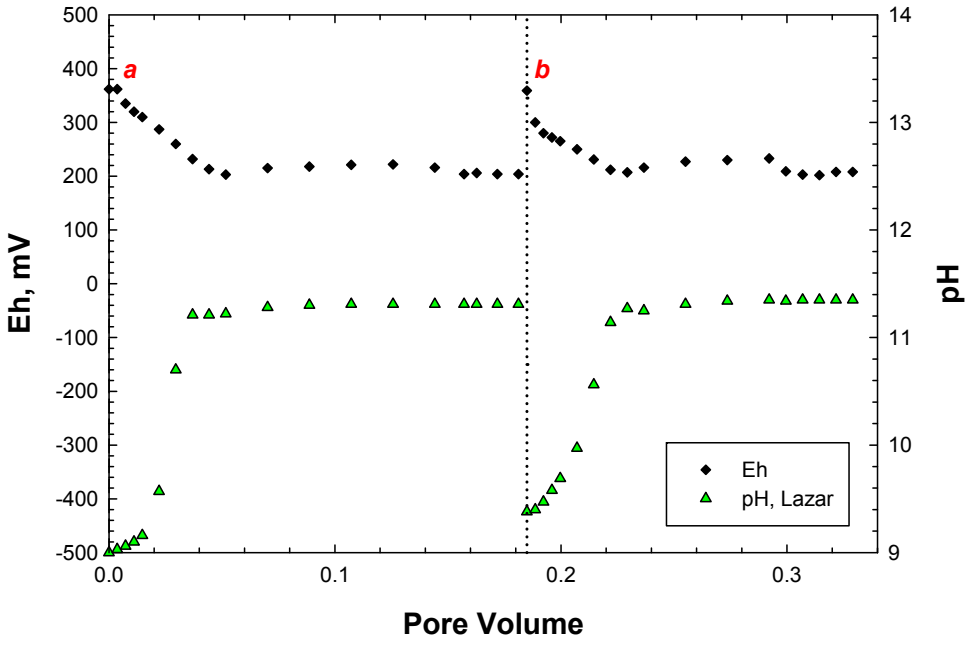

Figure 3-20. Measured Cell 2 Eh and pH Data as a Function of Number of Pore Volumes After Flow to the Column Was Resumed. Flow Was Stopped for 11 and 14 Days, Respectively, for the (a) and (b) Data.

solution in the Teflon tubing downstream of the grout column. As the solution that exited the column started to reach the microflow-through Eh and pH electrodes, the Eh quickly decreased to a steady state value of ~205 mV and the pH increased to a steady state value of ~11.3. The steady state Eh of ~205 mV is lower than the value (~290 mV) before the flow was stopped. In contrast, the steady state pH of ~11.3 is close to the value (~11.4) before the flow was stopped. The measured technetium concentrations of the two samples taken during the stopped-flow tests are 5.9×10^{-8} and 8.6×10^{-8} molar, which are higher than that of the last sample taken before the flow was interrupted [1.5×10^{-8} molar; Figure 19(b)]. The data indicate that the longer reaction time enabled a higher concentration of technetium to be released from the reducing grout. A lower solution Eh was attained due to the longer reaction time with the reducing grout.

3.2.3 Technetium and Selenium Speciation and Solubility Diagrams

An Eh-pH diagram illustrating technetium speciation is presented in Figure 3-21. The diagram was calculated using Geochemist's Workbench ACT2 Version 7.0 and the thermodynamic database thermo.com.v8.r6+.dat. Sulfate ion activity was set to 1×10^{-3} to represent the range of experimental sulfate concentrations [Figure 3-11(a)], and pertechnetate (TcO_4^-) ion activity was set to 1×10^{-8}. Values of experimental (Cell 1) Eh and pH also are plotted in the figure. Figure 3-21 indicates that the experimental system chemistry started under Eh conditions (~−400 mV) in which technetium solubility is low, constrained by the solubility of the Tc_3O_4 phase. As illustrated in Figure 3-22, which shows technetium activity in solution (approximately equal to technetium concentration at dilute concentrations) vs. pH and Eh, Tc_3O_4 solubility at pHs <13 is low (<10^{-8} molal) when Eh is equal to −350 mV, but is high (up to 0.10 molal) when Eh is equal to −250 mV.

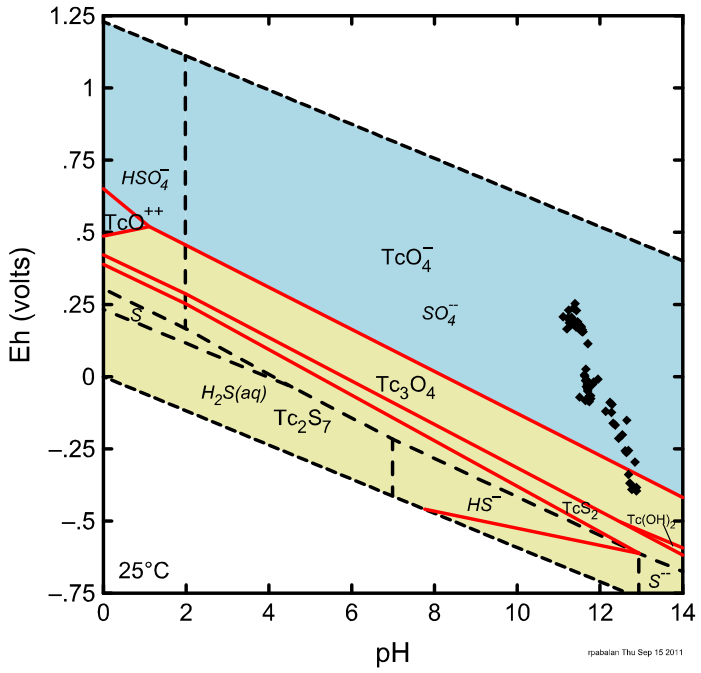

Figure 3-21. Eh–pH Diagram of Technetium Speciation Calculated Using Geochemist's Workbench ACT2 (TcO_4^- Activity = 10^{-8}; SO_4^{2-} Activity = 10^{-3}). Diamond Symbols Are Experimental Eh and pH Values From Figure 3-9. Upper and Lower Dashed Lines Bound the Water Stability Field. Other Dashed Lines Delineate the Sulfur Species Stability Fields.

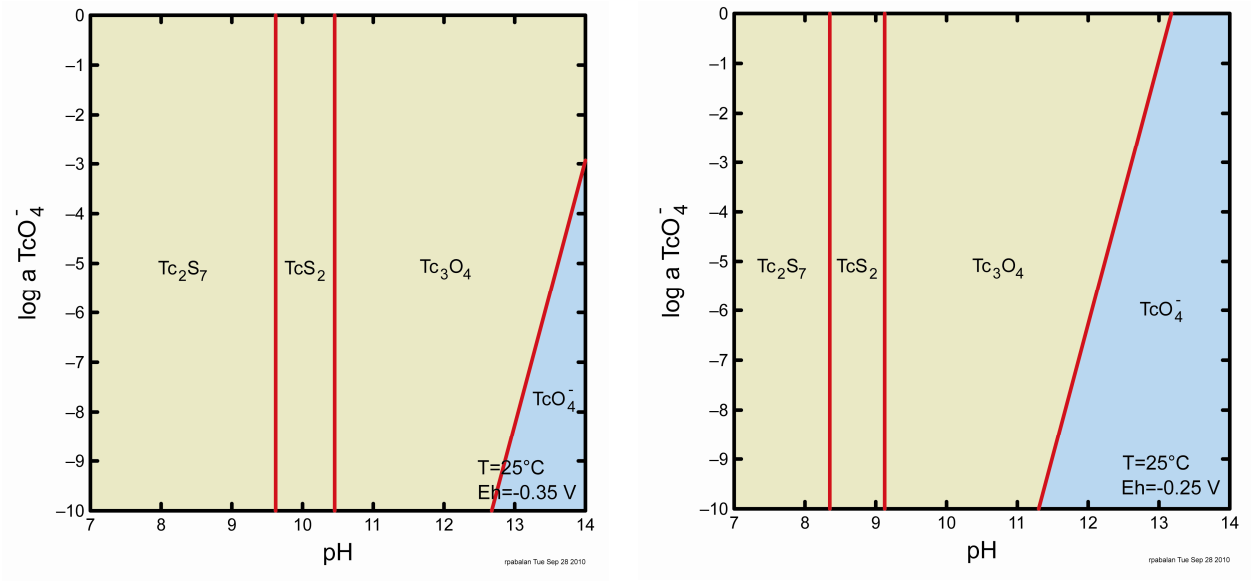

Figure 3-22. Technetium Solubility at 25 °C [77 °F] As a Function of pH at Eh Values of (a) –350 and (b) –250 mV Calculated Using Geochemist's Workbench ACT2 (SO_4^{2-} Activity = 10^{-3})

The system chemistry in Cell 1 evolved in less than 2 pore volumes to slightly lower pH but significantly higher Eh (–325 mV or higher) into the stability field of the pertechnetate ion. This transition should have corresponded to a significant increase in technetium release. However, data in Figures 3-9 and 3-12 show that up to 52 pore volumes, technetium release was relatively small and constant even though the system Eh was in the pertechnetate ion stability field. The time lag between Eh increase and technetium release possibly is due to slow oxidation of technetium at depth within the grout particles, which in turn is likely controlled by oxygen diffusion into the particles.

An alternative explanation is that technetium may have remained in the relatively insoluble Tc(IV) oxidation state even though the measured system Eh indicates that Tc(VII) would be thermodynamically favored. Some published studies indicate that certain forms or occurrences of Tc(IV) can be exceedingly resistant to oxidative remobilization (Fredrickson, et al., 2009). Studies by Wharton, et al. (2000) and Liu, et al. (2008) showed that TcO_4^- ions can be effectively reduced and coprecipitated by FeS_2, forming a TcS_2-like product, but that reoxidation of the FeS_2 host with aging resulted in technetium forming a TcO_2-like phase, rather than being oxidized back to the TcO_4^- ion.

Selenium release from the Cell 2 reducing grout was markedly different from that of technetium and likely involved a different release mechanism. Figure 3-23 shows an Eh–pH diagram of selenium speciation and the Cell 2 Eh and pH measurements. The figure indicates that under the initial Eh–pH conditions, selenium likely was present as an aqueous HSe^- species and its release would not have been solubility limited. Although selenium metal could precipitate as the Eh increased and, thus, inhibit selenium release, selenium metal stability is limited to a narrow range of Eh and its formation may have been too slow to significantly hinder selenium release.

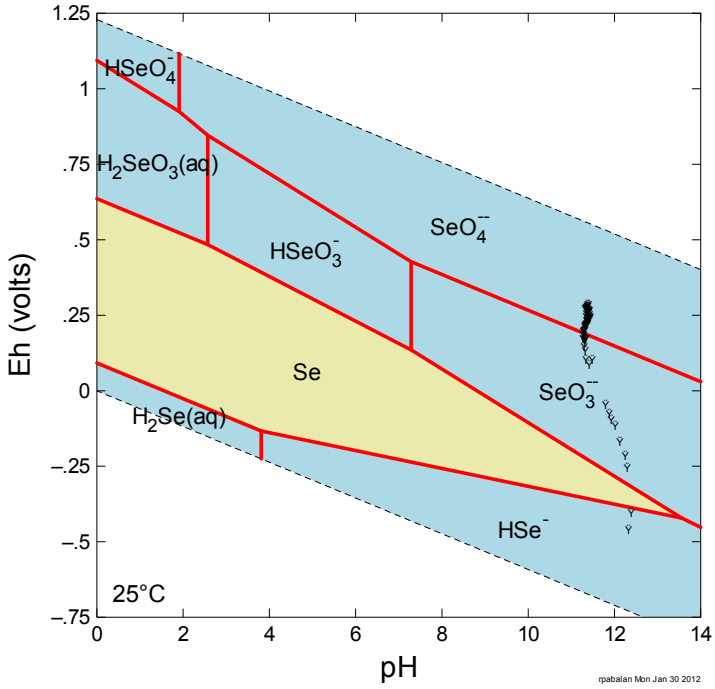

Figure 3-23. Eh–pH Diagram of Selenium Speciation Calculated Using Geochemist's Workbench ACT2 (SeO_3^{2-} Activity = 10^{-7}). Diamond Symbols Are Experimental Eh and pH Values From Figure 3-16. Upper and Lower Dashed Lines Bound the Water Stability Field.

3.3 Grout Cylinder Leaching Experiment Results

The technetium, selenium, nitrate, and nitrite leaching data are plotted as cumulative fractions leached versus time in Figures 3-24 and 3-25 (for grout cylinders cured at room temperature) and in Figures 3-26 and 3-27 {for grout cylinders cured at 60 °C [140 °F]}. Sodium leaching data for grout cylinders cured at room temperature and at 60 °C [140 °F] are plotted in Figure 3-28. Uranium results were not plotted, because the measured uranium concentrations were mostly below the ICP–MS detection limit (0.002 ppm). Qualitatively, the data indicate that the leach rates for the different species increase in the order technetium < nitrate ≈ nitrite < selenium < sodium.

Data analysis of the leaching data was coupled with a mechanistic model to determine the leaching mechanism(s) and to provide a basis, within certain constraints, for long-term predictions of contaminant release. The modeling approach and computer program [Accelerated Leach Test (ALT) Computer Program] used are described in Fuhrmann, et al. (1990). The solid lines in Figures 3-24 to 3-28 represent a diffusion model fitted to the data using the ALT program. The D_e values for each species were calculated using the ALT code based on the fraction leached and the shape of the curve fitted through the cumulative fraction leached data. The derived effective diffusion coefficient (D_e), which accounts for porosity, tortuosity, and sorption, is listed at the bottom of each graph and summarized in Table 3-4. The leaching data were generally consistent with a diffusion release mechanism,[6] with D_e values on the order of 10^{-11} cm^2/s [1.6×10^{-12} in^2/s] for technetium, nitrate, and nitrite; approximately 10^{-10} cm^2/s [1.6×10^{-11} in^2/s] for selenium; and approximately 10^{-9} cm^2/s [1.6×10^{-10} in^2/s] for sodium. The nitrate, nitrite, selenium, and sodium D_e values are higher for the grout cylinders cured at 60 °C [140 °F] compared to those cured at room temperature, but the technetium D_e value is lower for the former than for the latter.

For comparison, Gerdes, et al. (2007) reported a technetium D_e value of 4.8×10^{-12} cm^2/s [7.4×10^{-13} in^2/s] in saltstone grout and Pierce, et al. (2010) reported technetium D_e values in the range 1.2×10^{-11} to 2.3×10^{-13} cm^2/s [1.9×10^{-12} to 3.6×10^{-14} in^2/s] in grout with a composition similar to that of saltstone. Langton (1987) reported D_e values of 8×10^{-12} and 8×10^{-7} cm^2/s [1.2×10^{-12} and 1.2×10^{-7} in^2/s], respectively, for technetium and nitrate in saltstone grout. The much higher nitrate D_e value Langton (1987) reported compared to that derived from this study is due mostly to the difference in the microstructure of the grouts used inthe two studies. The grout Langton (1987) used had a water-to-cementitious-material weight ratio of 2.68, whereas the grout used in this study had a water-to-cement ratio of 0.6. Langton's (1987) grout had a very coarse pore structure that allowed faster nitrate diffusion compared to the grout used in this study. The technetium D_e value derived from this study is relatively close to the values Langton (1987), Gerdes, et al. (2007), and Pierce, et al. (2010) derived because technetium retention involves chemical stabilization (reduction and precipitation) and is not as affected by the grout pore structure compared to nitrate retention.

The ALT computer program has the ability to extrapolate future releases from full-scale waste forms (Fuhrmann, et al., 1990). This ability may provide support for predictions of long-term contaminant release, provided that the modeling results do not extend beyond certain

[6]Although the experimental data were fitted well with a diffusion equation, technetium that is released from the simulated saltstone likely must first be mobilized by a chemical reaction (e.g., oxidative dissolution) and then diffused through the encapsulating matrix. The ALT program has no option to consider a coupled reaction–diffusion reaction, but Ebert (2010) gives coupled reaction–diffusion equations that can be used to fit the contaminant release data.

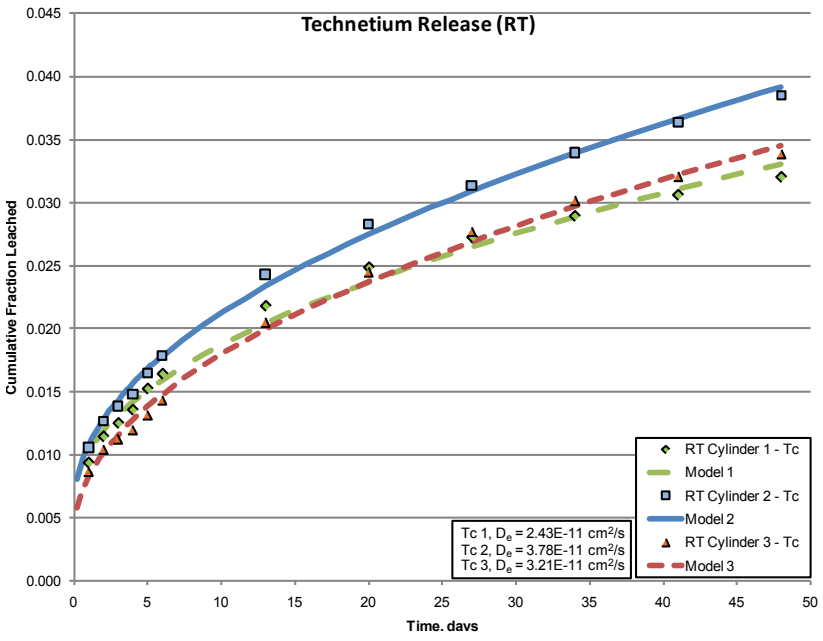

(a)

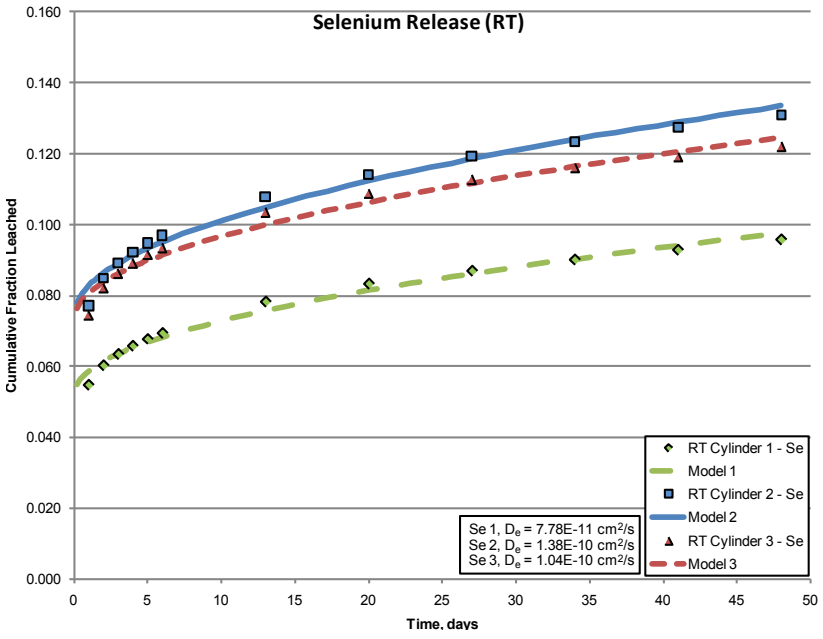

(b)

Figure 3-24. Cumulative Fraction Leached Versus Time of (a) Technetium and (b) Selenium From Three Simulated Saltstone Cylinders Cured at Room Temperature. The Symbols Represent Experimental Data, and The Curves Represent Diffusion Model Fits to the Data. The Derived Effective Diffusion Coefficients (D_eValues) Also Are Shown.

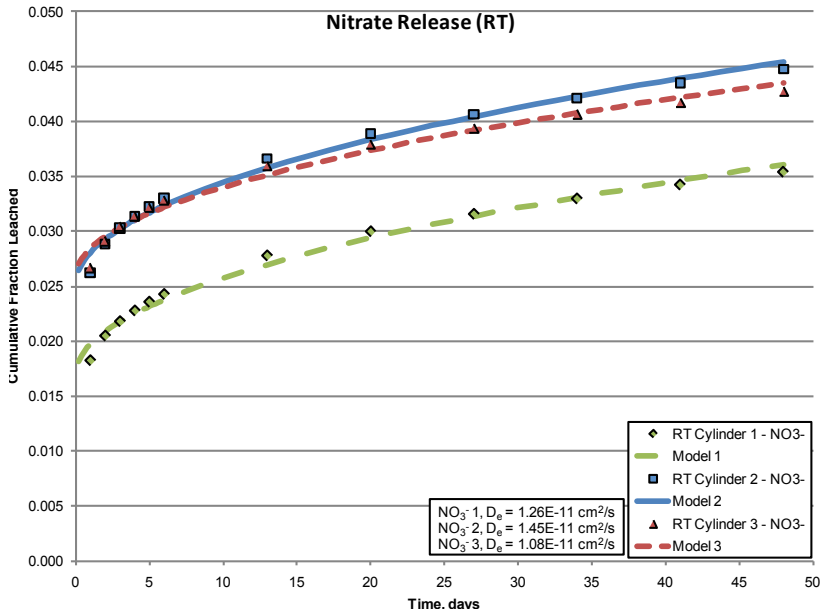

(a)

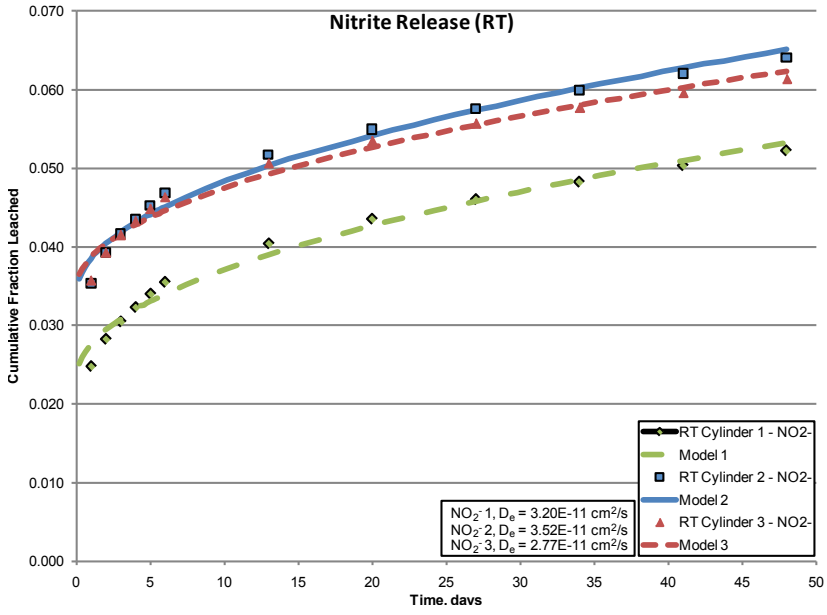

(b)

Figure 3-25. Cumulative Fraction Leached Versus Time of (a) Nitrate and (b) Nitrite From Three Simulated Saltstone Cylinders Cured at Room Temperature. The Symbols Represent Experimental Data, and The Curves Represent Diffusion Model Fits to the Data. The Derived Effective Diffusion Coefficients (D_e Values) Also Are Shown.

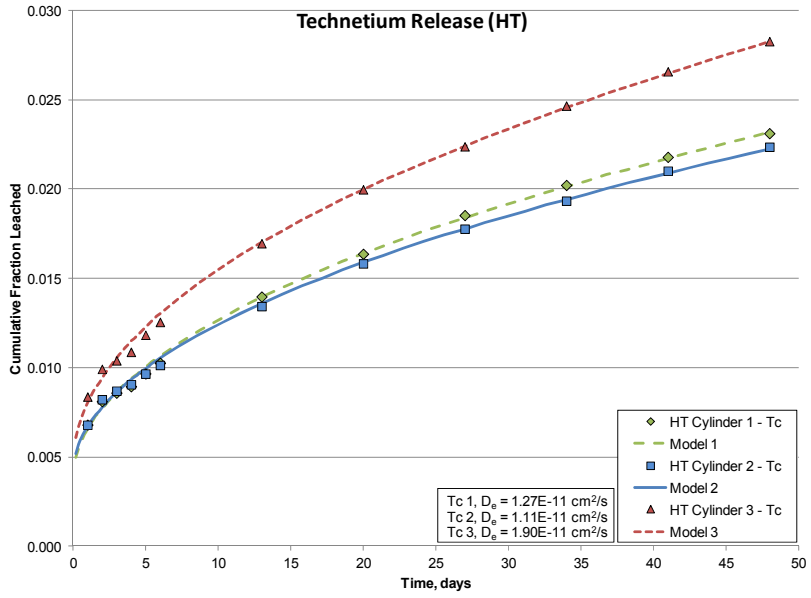

(a)

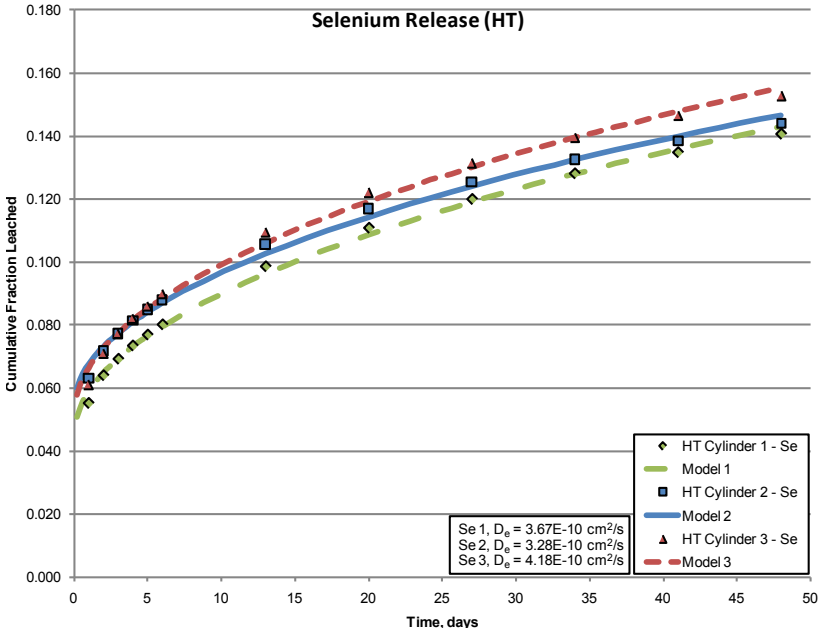

(b)

Figure 3-26. Cumulative Fraction Leached Versus Time of (a) Technetium and (b) Selenium From Three Simulated Saltstone Cylinders Cured at 60 °C [140 °F]. The Symbols Represent Experimental Data, and The Curves Represent Diffusion Model Fits to the Data. The Derived Effective Diffusion Coefficients (D_e Values) Also Are Shown.

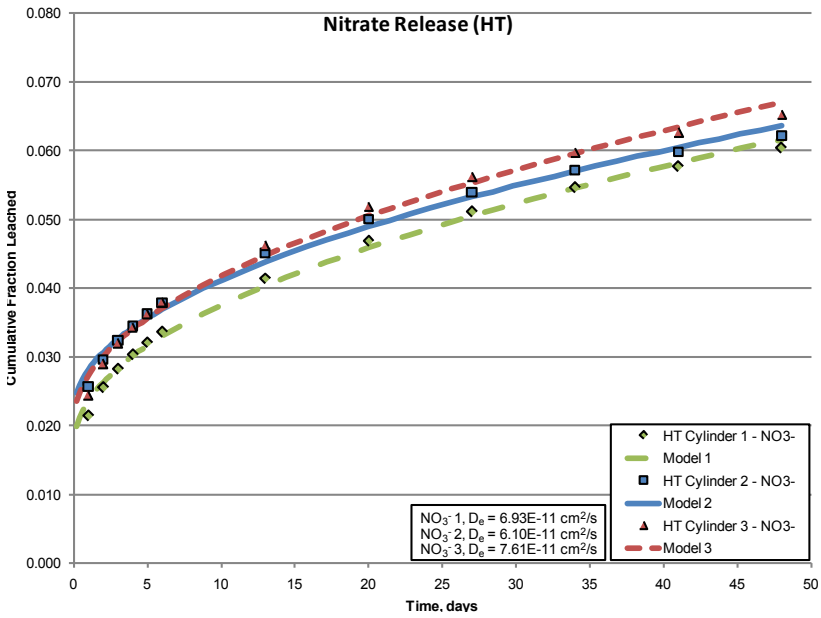

(a)

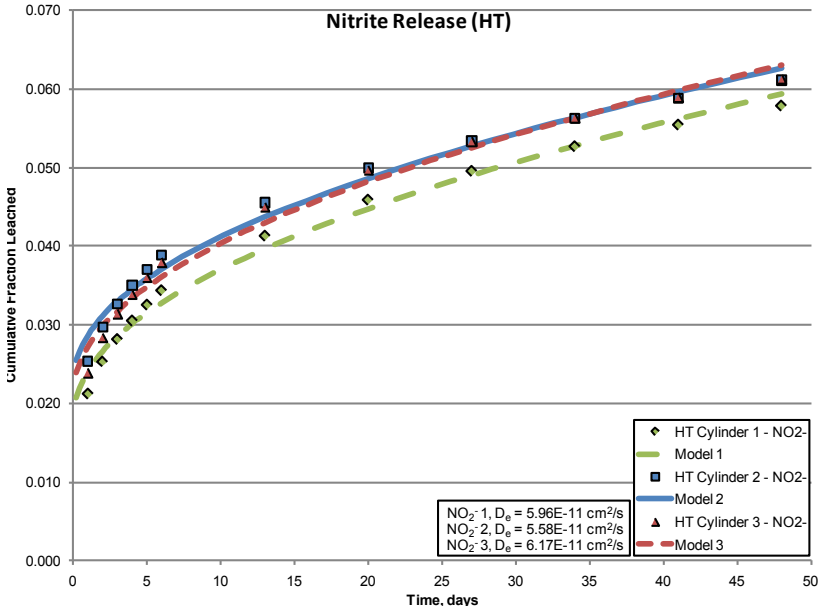

(b)

Figure 3-27. Cumulative Fraction Leached Versus Time of (a) Nitrate and (b) Nitrite From Three Simulated Saltstone Cylinders Cured at 60 °C [140 °F]. The Symbols Represent Experimental Data, and The Curves Represent Diffusion Model Fits to the Data. The Derived Effective Diffusion Coefficients (D_e Values) Also Are Shown.

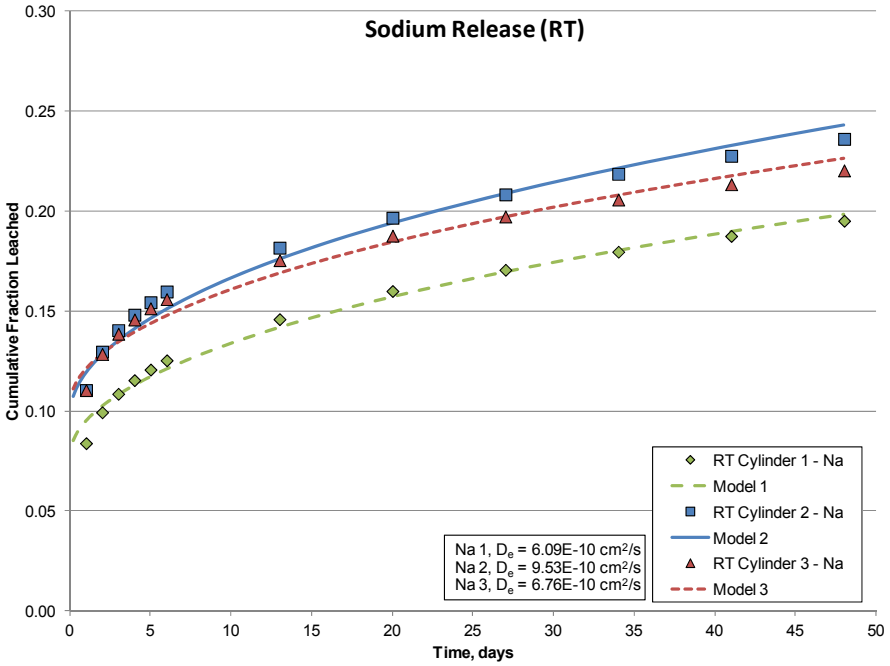

(a)

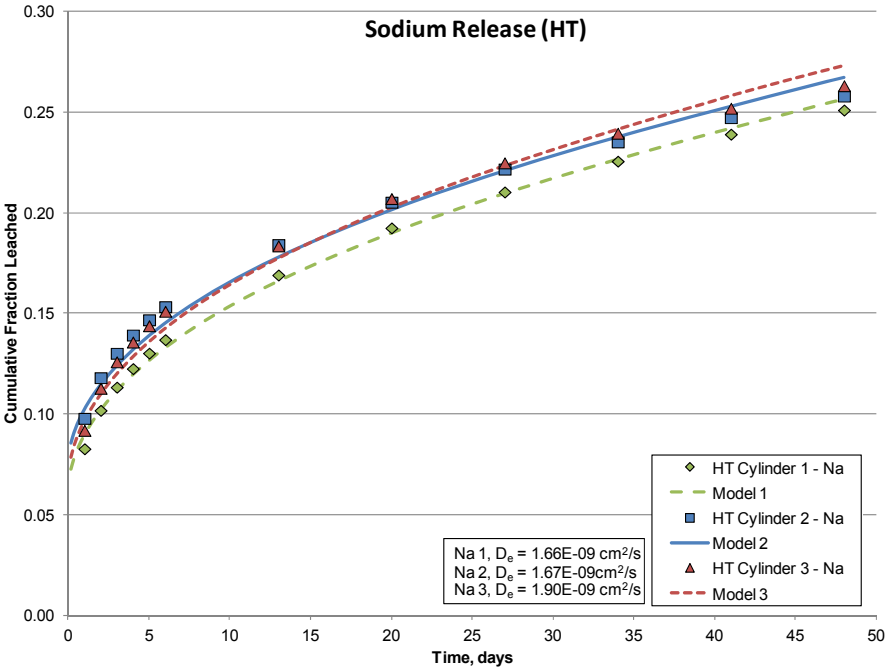

(b)

Figure 3-28. Cumulative Fraction Leached Versus Time of Sodium From Three Simulated Saltstone Cylinders Cured at (a) Room Temperature and (b) 60 °C [140 °F]. The Symbols Represent Experimental Data, and the Curves Represent Diffusion Model Fits to the Data. The Derived Effective Diffusion Coefficients (D_e Values) Also Are Shown.

Table 3-4. Effective Diffusion Coefficient (D_e) Derived From Grout Cylinder Leach Test Data Using the ALT Program*		
	Grout Curing Temperature	
Species	**Room Temperature**	**60 °C [140 °F]**
Technetium	$3.14 \pm 0.68 \times 10^{-11}$ cm^2/s	$1.43 \pm 0.42 \times 10^{-11}$ cm^2/s
Selenium	$1.07 \pm 0.30 \times 10^{-10}$ cm^2/s	$3.71 \pm 0.19 \times 10^{-10}$ cm^2/s
Sodium	$7.46 \pm 1.82 \times 10^{-10}$ cm^2/s	$1.74 \pm 0.14 \times 10^{-9}$ cm^2/s
Nitrate	$1.26 \pm 0.19 \times 10^{-11}$ cm^2/s	$6.88 \pm 0.76 \times 10^{-11}$ cm^2/s
Nitrite	$3.16 \pm 0.38 \times 10^{-11}$ cm^2/s	$5.90 \pm 0.30 \times 10^{-11}$ cm^2/s
*Average and standard deviation of data for three cylinders		

constraints. Limitations associated with scaling from short-term laboratory accelerated leach tests to long-term field predictions should be carefully considered. These limitations include (i) variability between laboratory and field samples, (ii) uncertainty in the evolution of the waste form (e.g., crack formation, changes in pore structure), (iii) uncertainty in the chemical composition of the infiltrate, (iv) uncertainty in the rate and nature of flow through the system (e.g., matrix vs. fracture flow) that affects leach rates, and (v) uncertainty in the amount of oxygen input to the system.

4 SUMMARY AND CONCLUSIONS

Two types of experiments were conducted to determine the release behavior of the redox-sensitive radioelements technetium, uranium, and selenium initially sequestered in reducing grout as water interacted with the grout and changed the system chemistry. One type of experiment flowed oxygen-bearing simulated SRS groundwater through a column of crushed and sieved simulated SRS saltstone material and monitored the changes in pH, Eh, and aqueous concentrations. Results from this experiment showed that significant changes in system chemistry occurred during the first 10 to 14 pore volumes of flow through the column. The effluent solution pH decreased relatively quickly from 12.9 to ~11.8 during the first 14 pore volumes, then decreased much more slowly, reaching only ~11.2 after 134 pore volumes. No pH buffering at 12.5 was observed, indicating portlandite did not form in significant amounts in the grout to buffer the pH at that value. The Eh quickly increased from a low value of –453 mV to positive Eh values as early as 12 pore volumes of solution flow, then increased more gradually afterward. In one of the two column experiments (Cell 1), a sudden 120-mV increase in Eh was observed after 46 pore volumes, but this sudden Eh increase was not observed in the other column experiment (Cell 2).

Technetium release from the simulated saltstone increased sharply during the first 10 pore volumes, increased more gradually until 52 pore volumes in Cell 1 or 26 pore volumes in Cell 2, then afterwards increased significantly with increasing pore volume. The technetium that was released early likely represents technetium that was not effectively immobilized in the reducing grout or technetium that was reoxidized during the crushing and sieving of the grout material. The significant increase in technetium release observed in Cell 1 after 52 pore volumes and in Cell 2 after 26 pore volumes is slightly delayed relative to the Eh increase observed in both cells. The technetium cumulative fraction leached from Cell 1 was 0.04 at 52 pore volumes, but increased to 0.25 at 134 pore volumes. The technetium cumulative fraction leached from Cell 2 was 0.10 at 26 pore volumes and increased to 0.19 at 132 pore volumes. The data show that uranium is retained in the reducing grout, whereas almost all of the selenium is released after 132 pore volumes. A posttest analysis of the Cell 1 grout that was extruded from the flow cell indicated that the fraction of technetium leached from the grout decreased from ~0.64 near the column inlet to ~0.46 near the column outlet. These values are higher than the Cell 1 value of 0.25 at 134 pore volumes that was derived from the technetium concentration in the effluent solutions, probably because the periodic sampling of effluent solutions may have missed short periods of high technetium fractional release, such as during the onset of the experiment or following the Eh transition. Notwithstanding the differences in the calculated technetium leached fraction, the data indicate that much of the technetium originally present in the column remained in a reduced, low solubility phase. This is consistent with a mass balance analysis that showed the amount of dissolved O_2 which has flowed through the column would have consumed only a fraction of the reducing capacity of the grout.

An Eh–pH diagram indicates the system chemistry in the column experiment started under conditions in which technetium solubility is low, constrained by Tc_3O_4 solubility, but eventually transitioned into the stability field of the pertechnetate ion. Although this transition should have corresponded to a significant increase in technetium release, it was not observed in the experiment. Instead, an increase in technetium release occurred later than the observed Eh increase and at a slower rate than expected based on the change in solution chemistry. The time lag between Eh increase and technetium release possibly is due to slow oxidation of technetium at depth within the grout particles, which in turn is likely controlled by oxygen diffusion into the particles. Based on literature information, an alternative explanation is the formation of a low solubility, likely metastable Tc(IV) phase that is resistant to oxidative

remobilization. In contrast to technetium, selenium release was not solubility limited. An Eh–pH diagram of selenium speciation indicates that under the initial Eh–pH conditions, selenium likely was present as an aqueous HSe^- species. Given that selenium release does not appear to be transport limited, release of technetium, once soluble, also is unlikely to be transport limited.

The second type of experiment leached cylindrical specimens of simulated saltstone material—one set cured at room temperature and another at 60 °C [140 °F]—in deionized water and monitored aqueous concentrations over time. Qualitatively, the data indicate that the leach rates for the different species increase in the order technetium < nitrate ≈ nitrite < selenium < sodium. Measured uranium concentrations were mostly below the ICP–MS detection limit, indicating uranium was not released from the reducing grout within the timeframe of the experiment. Data analysis using the ALT computer program indicated the leaching data were generally consistent with a diffusion release mechanism. A more likely release mechanism involves both chemical reaction (e.g., oxidative dissolution) and diffusion, but the ALT program has no option to consider such mechanism. D_e values on the order of 10^{-11} cm^2/s [1.6×10^{-12} in^2/s] were derived for technetium, nitrate, and nitrite, approximately 10^{-10} cm^2/s [1.6×10^{-11} in^2/s] for selenium, and approximately 10^{-9} cm^2/s [1.6×10^{-10} in^2/s] for sodium. The nitrate, nitrite, selenium, and sodium D_e values are higher for the grout cylinders cured at 60 °C [140 °F] compared to those cured at room temperature, but the technetium D_e is lower for the former than for the latter.

Due to the limited spatial and temporal scale and range of parameters (e.g., particle or monolith size, flow rate) used in the experiments, care should be taken when extrapolating the results to actual field conditions. A full-scale system will have flow geometries, flow rates, and reactive surface areas that will vary spatially and temporally. Reaction kinetics also will affect the evolution of the system chemistry. To enable extrapolation of experimental results to longer time frames and larger spatial scales, as well as facilitate an evaluation of the effect of varying chemical (e.g., solution composition) and physical (e.g., particle size, surface area, flow rate) parameters on contaminant release, reactive transport modeling of contaminant leaching could be conducted. As the range of parameters in these experiments was limited, additional experiments varying the particle size and/or flow rate would be useful. In addition, because the physical and chemical conditions in actual saltstone waste and the release behavior of radionuclides could be different than those in the laboratory experiments, leaching experiments using actual SRS saltstone samples are strongly recommended.

5 REFERENCES

Allen, P.G., G.S. Siemering, D.K. Shuh, J.J. Bucher, N.M. Edelstein, C.A. Langton, S.B. Clark, T. Reich, and M.A. Denecke. "Technetium Speciation in Cement Waste Forms Determined by X-Ray Absorption Fine Structure Spectroscopy." *Radiochimica Acta*. Vol. 76. pp. 77–86. 1997.

Aloy, A., E.N. Kovarskaya, J.R. Harbour, C.A. Langton, and E.W. Holtzscheiter. "Pretreatment of Tc-Containing Waste and Its Effect on Tc-99 Leaching From Grouts." Scientific Basis for Nuclear Waste Management XXX. Proceedings of the Materials Research Society Symposium. Vol. 985. D.S. Dunn, C. Poinssot, and B. Begg, eds. Warrendale, Pennsylvania: Materials Research Society. 2007.

Angus, M.J. and F.P. Glasser. "The Chemical Environment in Cement Matrices." Scientific Basis for Nuclear Waste Management IX. Proceedings of the Materials Research Society Symposium Vol. 50. L.O. Werme, ed. Warrendale, Pennsylvania: Materials Research Society. 1985.

ASTM International. ASTM C–1308–95, "Standard Test Method for Accelerated Leach Test for Diffusive Releases From Solidified Waste and a Computer Program To Model Diffusive, Fractional Leaching from Cylindrical Waste Forms." West Conshohocken, Pennsylvania: ASTM International. 2001.

Atkins, M. and F.P. Glasser. "Application of Portland Cement-Based Materials to Radioactive Waste Immobilization." *Waste Management*. Vol. 12. pp. 105–131. 1992.

Brodda, B.G. "Leachability of Technetium From Concrete." *The Science of the Total Environment*. Vol. 69. pp. 319–345. 1988.

Cook, J.R. and J.R. Fowler. "Radiological Performance Assessment for the Z-Area Disposal Facility (U)." WSRC–RP–92–1360. Rev. 0. Aiken, South Carolina: Westinghouse Savannah River Company. 1992.

Deer, W.A., R.A. Howie, and J. Zussman. *An Introduction to the Rock-Forming Minerals*. London, United Kingdom: Longman Group Limited. 1966.

Denham, M.E. "Estimation of Eh and pH Transitions in Pore Fluids During Aging of Saltstone and Disposal Unit Concrete." SRNL–TR–2008–00283. Aiken, South Carolina: Savannah River National Laboratory. 2008.

DOE-Idaho. DOE/ID–10966, "Performance Assessment for the Tank Farm Facility at the Idaho National Engineering and Environmental Laboratory." Rev. 1. Idaho Falls, Idaho: DOE-Idaho. 2003.

Ebert, W.L. NUREG/CR–7025, "Radionuclide Release from Slag and Concrete Waste Materials. Part 1: Conceptual Models of Leaching from Complex Materials and Laboratory Test Methods." Washington, DC: U.S. Nuclear Regulatory Commission. 2010.

Ewart, F.T., J.L. Smith-Briggs, H.P. Thomason, and S.J. Williams. "The Solubility of Actinides in a Cementitious Near-field Environment." *Waste Management*. Vol. 12. pp. 241–252. 1992.

Fredrickson, J.K., J.M. Zachara, A.E. Plymale, S.M. Heald, J.P. McKinley, D.W. Kennedy, C. Liu, and P. Nachimuthu. "Oxidative Dissolution Potential of Biogenic and Abiogenic TcO_2 in Subsurface Sediments." *Geochimica et Cosmochimica Acta*. Vol. 73. pp. 2,299–2,313. 2009.

Fuhrmann, M., J. Heiser, R.F. Pietrzak, E.M. Franz, and P. Colombo. "Accelerated Leach Test Method and Users' Guide for the ALT Computer Program." BNL–52267. Upton, New York: Brookhaven National Laboratory. 1990.

Gerdes, K.D., J.R. Harbour, J.C. Marra, D.K. Peeler, T.B. Calloway, J.A. Roach, J.D. Vienna, A.S. Aloy, S.V. Stefanovsky, and M.D. Bondarkov. "The U.S. Department of Energy–Office of Environmental Management's International Program." Waste Management '07 Conference, Tucson, Arizona, February 15–March 1, 2007. Washington, DC. U.S. Department of Energy, Office of Environmental Management. 2007.

Gilliam, T.M., R.D. Spence, B.S. Evans-Brown, I.L. Morgan, J.L. Shoemaker, and W.D. Bostock. "Performance Testing of Blast Furnace Slag for Immobilization of Technetium in Grout." Proceedings from Spectrum '88—International Topical Meeting on Nuclear and Hazardous Waste Management, Pasco, Washington, September 11–15, 1988. LaGrange, Illinois: American Nuclear Society. 1988.

Harbour, J.R., T.B. Edwards, and V.J. Williams. "Impact of Time/Temperature Curing Conditions and Aluminate Concentration on Saltstone Properties." SRNL-STI-2009-00184. Aiken, South Carolina: Savannah River National Laboratory. 2009.

Kaplan, D.I., K. Roberts, J. Coates, M. Siegfried, and S. Serkiz. "Saltstone and Concrete Interactions With Radionuclides: Sorption (K_d), Desorption, and Reduction Capacity Measurements." SRNS–STI–2008–00045. Aiken, South Carolina: Savannah River National Laboratory. 2008.

Kaplan, D.I. and T. Hang. "Estimated Duration of the Subsurface Reduction Environment Produced by the Saltstone Disposal Facility on the Savannah River Site." Rev. 0. WSRC–STI–2007–00046. Aiken, South Carolina: Westinghouse Savannah River Company. 2007.

Kaplan, D.I., T. Hang, and S.E. Aleman. "Estimated Duration of the Reduction Capacity Within a High-Level Waste Tank (U)." Rev. 0. WSRC–RP–2005–01674. Aiken, South Carolina: Westinghouse Savannah River Company. 2005.

Langton, C.A. "Slag-Based Saltstone Formulations." DP–MS–87–95. Aiken, South Carolina: Savannah River Laboratory. 1987.

Liu, Y., J. Terry, and S. Jurisson. "Pertechnetate Immobilization With Amorphous Iron Sulfide." *Radiochimica Acta*. Vol. 96. pp. 823–833. 2008.

———. "Pertechnetate Immobilization in Aqueous Media With Hydrogen Sulfide Under Anaerobic and Aerobic Environments." *Radiochimica Acta*. Vol. 95. pp. 717–725. 2007.

Lukens, W.W., J.I. Bucher, D.K. Shuh, and N.M. Edelstein. "Evolution of Technetium Speciation in Reducing Grout." *Environmental Science and Technology*. Vol. 39. pp. 8,064–8,070. 2005.

Pabalan, R.T., F.P. Glasser, D.A. Pickett, G.R. Walter, S. Biswas, M.R. Juckett, L.M. Sabido, and J.L. Myers. "Review of Literature and Assessment of Factors Relevant to Performance of Grouted Systems for Radioactive Waste Disposal." CNWRA 2009-001. San Antonio, Texas: Center for Nuclear Waste Regulatory Analyses. 2009.

Painter, S.L. and R.T. Pabalan. "Estimated Longevity of Reducing Environment in Grouted Systems for Radioactive Waste Disposal." San Antonio, Texas: Center for Nuclear Waste Regulatory Analyses. 2009.

Pickett, D., K.E. Pinkston, and J.L. Myers. "Assessing Radionuclide Solubility Limits for Cement-Based, Near-Surface Disposal." Scientific Basis for Nuclear Waste Management XXXII. Paper No. 1124–Q07–19. R.B. Rebak, N.C. Hyatt, and D.A. Pickett, eds. Warrendale, Pennsylvania: Materials Research Society. 2009.

Pierce, E.M., W. Um, K.J. Cantrell, M.M. Valenta, J.M. Westsik Jr., R.J. Serne, and K.E. Parker. "Secondary Waste Form Screening Test Results—Cast Stone and Alkali Alumino-Silicate Geopolymer." PNNL–19505. Richland, Washington: Pacific Northwest National Laboratory. 2010.

Roberts, K. and D.I. Kaplan. "Reduction Capacity of Saltstone and Saltstone Components." SRNL–STI–2009–00637. Rev. 0. Aiken, South Carolina: Savannah River National Laboratory. 2009.

Savannah River Remediation Closure and Waste Disposal Authority. "Performance Assessment for the Saltstone Disposal Facility at the Savannah River Site." SRR–CWDA–2009–00017. Rev. 0. Aiken, South Carolina: Savannah River Remediation Closure and Waste Disposal Authority. 2009.

Strom, R.N. and D.S. Kaback. "SRP Baseline Hydrogeologic Investigation: Aquifer Characterization, Groundwater Geochemistry of the Savannah River Site and Vicinity." WSRC–RP–92–450. Aiken, South Carolina: Westinghouse Savannah River Company. 1992.

Wharton, M.J., B. Atkins, J.M. Charnock, F.R. Livens, R.A.D. Pattrick, and D. Collison. "An X-ray Absorption Spectroscopy Study of the Coprecipitation of Tc and Re With Mackinawite (FeS)." *Applied Geochemistry*. Vol. 15. pp. 347–354. 2000.